Article

P Addition to Terminal Phosphide M#P Triple Bonds: A Rational Synthesis of *cyclo*-P Complexes

Nicholas A. Piro, and Christopher C. Cummins

J. Am. Chem. Soc., **2008**, 130 (29), 9524-9535 • DOI: 10.1021/ja802080m • Publication Date (Web): 28 June 2008

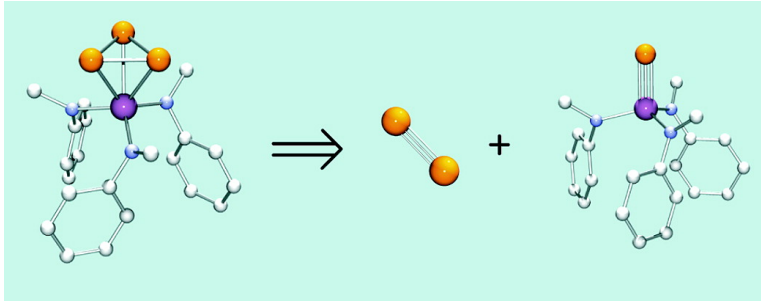

J|A|C|S
ARTICLES

Published on Web 06/28/2008

P_2 Addition to Terminal Phosphide M≡P Triple Bonds: A Rational Synthesis of *cyclo*-P_3 Complexes

Nicholas A. Piro and Christopher C. Cummins*

Department of Chemistry, Massachusetts Institute of Technology, 77 Massachusetts Avenue, Room 6-435, Cambridge, Massachusetts 02139

Received March 20, 2008; E-mail: ccummins@mit.edu

Abstract: The diphosphaazide complex (Mes*NPP)Nb(N[Np]Ar)$_3$ (Mes* = 2,4,6-tri-*tert*-butylphenyl, Np = neopentyl, Ar = 3,5-$Me_2C_6H_3$), **1**, has previously been reported to lose the P_2 unit upon gentle heating, to form (Mes*N)Nb(N[Np]Ar)$_3$, **2**. The first-order activation parameters for this process have been estimated here using an Eyring analysis to have the values $\Delta H^{\ddagger} = 19.6(2)$ kcal/mol and $\Delta S^{\ddagger} = -14.2(5)$ eu. The eliminated P_2 unit can be transferred to the terminal phosphide complexes P≡M(N[^{i}Pr]Ar)$_3$, **3**-M (M = Mo, W), and [P≡Nb(N[Np]Ar)$_3$]$^-$, **3**-Nb, to give the *cyclo*-P_3 complexes (P_3)M(N[^{i}Pr]Ar)$_3$ and [(P_3)Nb(N[Np]Ar)$_3$]$^-$. These reactions represent the formal addition of a P≡P triple bond across a M≡P triple bond and are the first efficient transfers of the P_2 unit to substrates present in stoichiometric quantities. The related complex (OC)$_5$W(Mes*NPP)Nb(N[Np]Ar)$_3$, **1**-W(CO)$_5$, was used to transfer the (P_2)W(CO)$_5$ unit in an analogous manner to the substrates **3**-M (M = Mo, W, Nb) as well as to [(OC)$_5$WP≡Nb(N[Np]Ar)$_3$]$^-$. The rate constants for the fragmentation of **1** and **1**-W(CO)$_5$ were unchanged in the presence of the terminal phosphide **3**-Mo, supporting the hypothesis that molecular P_2 and (P_2)W(CO)$_5$, respectively, are reactive intermediates. In a reaction related to the combination of P≡P and M≡P triple bonds, the phosphaalkyne AdC≡P (Ad = 1-adamantyl) was observed to react with **3**-Mo to generate the *cyclo*-CP_2 complex (AdCP_2)Mo(N[^{i}Pr]Ar)$_3$. Reactions of the electrophiles Ph_3SnCl, Mes*NPCl, and AdC(O)Cl with the anionic, nucleophilic complexes [(OC)$_5$W(P_3)Nb(N[Np]Ar)$_3$]$^-$ and [{(OC)$_5$W}$_2$(P_3)Nb(N[Np]Ar)$_3$]$^-$ yielded coordinated η^2-triphosphirene ligands. The Mes*NPW(CO)$_5$ group of one such product engages in a fluxional ring-migration process, according to NMR spectroscopic data. The structures of (OC)$_5$W(P_3)W(N[^{i}Pr]Ar)$_3$, [(Et_2O)Na][{(OC)$_5$W}$_2$-(P_3)Nb(N[Np]Ar)$_3$], (AdCP_2)Mo(N[^{i}Pr]Ar)$_3$, (OC)$_5$W(Ph_3SnP_3)Nb(N[Np]Ar)$_3$, Mes*NP(W(CO)$_5$)P_3Nb(N[Np]Ar)$_3$, and {(OC)$_5$W}$_2$AdC(O)P_3Nb(N[Np]Ar)$_3$, as determined by X-ray crystallography, are discussed in detail.

Introduction

The generation and reactivity of multiple bonds involving the heavier p-block elements is a field of considerable modern interest.[1–5] Underlying this intrigue is the weak propensity of these elements (relative to their lighter congeners) to engage in such bonding.[6] Exemplifying this dichotomy is a comparison of the stable allotropes of nitrogen and oxygen with those of phosphorus and sulfur. While the allotropes of the lighter elements, N_2 and O_2, possess triple and double bonds, respectively, the common molecular allotropes of the 3p elements are P_4 and S_8, which are constructed exclusively with single bonds.[7]

The use of unstable, multiply bonded allotropes of the heavier p-block elements as synthetic intermediates has significant precedent for sulfur.[8–18] One example of S_2 formation is the fragmentation of 9,10-epidithio-9,10-dihydroanthracene, where the formation of anthracene upon S_2 extrusion drives the reaction.[16,17] The reaction chemistry of singlet S_2 has been defined through trapping reactions,[19] with S_2 even finding synthetic use in drug synthesis.[20] In contrast to this, molecular diphosphorus has been studied primarily in the gas phase at

(1) Rivard, E.; Power, P. P. *Inorg. Chem.* **2007**, *46*, 10047–10064.
(2) Weber, L. *Chem. Rev.* **1992**, *92*, 1839–1906.
(3) Power, P. P. *Chem. Commun.* **2003**, 2091–2101.
(4) Power, P. P. *Chem. Rev.* **1999**, *99*, 3463–3503.
(5) Norman, N. C. *Polyhedron* **1993**, *12*, 2431–2446.
(6) Burdett, J. K. *Chemical Bonds: A Dialog*; Wiley: New York, 1997.
(7) Greenwood, N. N.; Earnshaw, A. *Chemistry of the Elements*, 2nd ed.; Butterworth-Heinemann: Oxford, U.K., 1997.
(8) Rakitin, O. A.; Rees, C. W.; Vlasova, O. G. *Tetrahedron Lett.* **1996**, *37*, 4589–4592.
(9) Gilchrist, T. L.; Wood, J. E. *J. Chem. Soc., Chem. Commun.* **1992**, 1460–1461.
(10) Steliou, K. *Acc. Chem. Res.* **1991**, *24*, 341–350.
(11) Steliou, K.; Salama, P.; Brodeur, D.; Gareau, Y. *J. Am. Chem. Soc.* **1987**, *109*, 926–927.
(12) Schmidt, M.; Görl, U. *Angew. Chem., Int. Ed. Engl.* **1987**, *26*, 887–889.
(13) Steliou, K.; Gareau, Y.; Harpp, D. N. *J. Am. Chem. Soc.* **1984**, *106*, 799–801.
(14) Harpp, D. N. *Phosphorus, Sulfur Silicon Relat. Elem.* **1997**, *120*, 41–59.
(15) Okuma, K.; Kuge, S.; Koga, Y.; Shioji, K.; Wakita, H.; Machiguchi, T. *Heterocycles* **1998**, *48*, 1519–1522.
(16) Ando, W.; Sonobe, H.; Akasaka, T. *Tetrahedron* **1990**, *46*, 5093–5100.
(17) Ando, W.; Sonobe, H.; Akasaka, T. *Tetrahedron Lett.* **1987**, *28*, 6653–6656.
(18) Harpp, D. N.; MacDonald, J. G. *J. Org. Chem.* **1988**, *53*, 3812–3814.
(19) The method of using butadiene and norbornene to assert the intermediacy of disulfur should be treated with caution; as discussed in: Micallef, A. S.; Bottle, S. E. *Tetrahedron Lett.* **1997**, *38*, 2303–2306.
(20) Steliou, K.; Gareau, Y.; Milot, G.; Salama, P. *Phosphorus, Sulfur Silicon Relat. Elem.* **1989**, *43*, 209–241.

10.1021/ja802080m CCC: $40.75

high temperatures or by matrix-isolation experiments.[21–27] For example, the equilibrium $P_4 \rightleftarrows 2P_2$ can be used to generate diphosphorus, but this equilibrium becomes important only at temperatures higher than 1100 K.[7] Recent work has focused on a new strategy for the ostensible generation and trapping of P_2 and the related tungsten pentacarbonyl adduct $(P_2)W(CO)_5$ in liquid media that uses the complex (Mes*NPP)Nb(N[Np]Ar)$_3$ (Mes* = 2,4,6-tri-*tert*-butylphenyl, Np = neopentyl, Ar = 3,5-$Me_2C_6H_3$), **1**.[28] This strategy utilizes a reaction analogous to that between an organic azide and a metal fragment to liberate N_2 and yield a metal imido.[29–38] This strategy entails the synthesis of an η^2-complexed diphosphaazide ligand (η^2-PPNR) atop a niobium tris(anilide) platform, resulting in a molecular system that is poised for P_2 extrusion to yield a strong niobium(V)−imido bond as the thermodynamic driving force.

We have reported previously on the trapping of proposed P_2 and $(P_2)W(CO)_5$ intermediates by organic dienes[28] and by a low-valent platinum complex.[39] However, these efforts to define a solution-phase chemistry of P_2-containing intermediates under readily achieved laboratory conditions have been plagued by the required large excess of the trapping reagent or by direct reactions between potential trapping reagents and the P_2-eliminating complex.[28,39] In the present work, we sought to further define the reaction chemistries of complex **1** and its tungsten pentacarbonyl adduct as sources of P_2 and further test the mechanistic hypothesis that P_2 and $(P_2)W(CO)_5$, respectively, are reactive, transient intermediates in these reactions. To this end, we have targeted the identification of a reactant class for trapping the putative P_2 and $(P_2)W(CO)_5$ intermediates that is capable of fulfilling the following criteria: (a) The trap should not react directly with complex **1**, a corollary to which is (b) that complex **1** should exhibit a unimolecular fragmentation rate constant that is independent of the identity or concentration of the trap. Also, it was desired (c) that the trap should be efficient, allowing it to be employed in stoichiometric quantities, in contrast with diene traps employed previously that had to be used in large excesses for efficient incorporation of P_2 into the double Diels−Alder product. Recognizing that prior trapping experiments, such as those involving organic dienes, resulted in consumption of 2 equiv of the trap per P_2 unit via a reaction cascade, we sought to simplify matters by requiring (d) that the trap be capable of reacting to completion with P_2 in a 1:1 ratio. We report herein that terminal metal phosphide complexes, as exemplified by P≡Mo(N[^{t}Pr]Ar)$_3$, **3**-Mo, satisfy the four criteria (a−d) articulated above.

Terminal metal phosphide complexes, i.e., species of the form P≡ML$_n$, were attractive candidates because the reaction between P_2 and P≡ML$_n$ was expected to afford MP_3 tetrahedra; viewed in another way, the product would contain the *cyclo*-P_3 moiety as a complexed ligand. The organometallic analogue of this transformation is the reaction between a terminal alkylidyne and an alkyne, which, in addition to the formation of metallacyclobutadienes,[40–42] can sometimes result in the formation of η^3-cyclopropenyl complexes.[43–46] Notably, trapping of P_2 by M≡P triple bonds can be considered as a possible mechanism for *cyclo*-P_3 complex formation in the course of P_4 activation by metal complexes.[47]

Additionally, while several *cyclo*-P_3 complexes have been reported in the literature, most were synthesized via white phosphorus (P_4) activation.[48–57] A few were assembled using reactions between P_2-bridged complexes and the P_1 synthons PCl_3 and PCl_5,[58] and a cluster containing a terminal (*cyclo*-P_3)Fe unit was isolated from the reaction of $FeCl_2$, LiCp*, and $P_7(SiMe_3)_3$.[59] A retrosynthetic analysis[60] of *cyclo*-P_3 complexes suggests that the simple combination of a P≡P triple bond with

(21) Stevenson, D. P.; Yost, D. M. *J. Chem. Phys.* **1941**, *9*, 403–408.
(22) Bock, H.; Müller, H. *Inorg. Chem.* **1984**, *23*, 4365–4368.
(23) Andrews, L.; McCluskey, M.; Mielke, Z.; Withnall, R. *J. Mol. Struct.* **1990**, *222*, 95–108.
(24) Mielke, Z.; McCluskey, M.; Andrews, L. *Chem. Phys. Lett.* **1990**, *165*, 146–154.
(25) McCluskey, M.; Andrews, L. *J. Phys. Chem.* **1991**, *95*, 2988–2994.
(26) Kornath, A.; Kaufmann, A.; Torheyden, M. *J. Chem. Phys.* **2002**, *116*, 3323–3326.
(27) Solouki, B.; Bock, H.; Haubold, W.; Keller, W. *Angew. Chem., Int. Ed. Engl.* **1990**, *29*, 1044–1046.
(28) Piro, N. A.; Figueroa, J. S.; McKellar, J. T.; Cummins, C. C. *Science* **2006**, *313*, 1276–1279.
(29) Abu-Omar, M. M.; Shields, C. E.; Edwards, N. Y.; Eikey, R. A. *Angew. Chem., Int. Ed.* **2005**, *44*, 6203–6207.
(30) Hillhouse, G. L.; Bercaw, J. E. *Organometallics* **1982**, *1*, 1025–1029.
(31) Osborne, J. H.; Rheingold, A. L.; Trogler, W. C. *J. Am. Chem. Soc.* **1985**, *107*, 7945–7952.
(32) Bart, S. C.; Lobkovsky, E.; Bill, E.; Chirik, P. J. *J. Am. Chem. Soc.* **2006**, *128*, 5302–5303.
(33) Thyagarajan, S.; Shay, D. T.; Incarvito, C. D.; Rheingold, A. L.; Theopold, K. H. *J. Am. Chem. Soc.* **2003**, *125*, 4440–4441.
(34) Castro-Rodriguez, I.; Olsen, K.; Gantzel, P.; Meyer, K. *J. Am. Chem. Soc.* **2003**, *125*, 4565–4571.
(35) Hanna, T. E.; Keresztes, I.; Lobkovsky, E.; Bernskoetter, W. H.; Chirik, P. J. *Organometallics* **2004**, *23*, 3448–3458.
(36) Proulx, G.; Bergman, R. G. *Organometallics* **1996**, *15*, 684–692.
(37) Proulx, G.; Bergman, R. G. *J. Am. Chem. Soc.* **1995**, *117*, 6382–6383.
(38) Fickes, M. G.; Davis, W. M.; Cummins, C. C. *J. Am. Chem. Soc.* **1995**, *117*, 6384–6385.
(39) Piro, N. A.; Cummins, C. C. *Inorg. Chem.* **2007**, *46*, 7387–7393.
(40) Churchill, M. R.; Ziller, J. W.; Freudenberger, J. H.; Schrock, R. R. *Organometallics* **1984**, *3*, 1554–1562.
(41) Freudenberger, J. H.; Schrock, R. R.; Churchill, M. R.; Rheingold, A. L.; Ziller, J. W. *Organometallics* **1984**, *3*, 1563–1573.
(42) Pedersen, S. F.; Schrock, R. R.; Churchill, M. R.; Wasserman, H. J. *J. Am. Chem. Soc.* **1982**, *104*, 6808–6809.
(43) Churchill, M. R.; Fettinger, J. C.; McCullough, L. G.; Schrock, R. R. *J. Am. Chem. Soc.* **1984**, *106*, 3356–3357.
(44) Churchill, M. R.; Ziller, J. W.; Pedersen, S. F.; Schrock, R. R. *J. Chem. Soc., Chem. Commun.* **1984**, 485–486.
(45) Schrock, R. R.; Murdzek, J. S.; Freudenberger, J. H.; Churchill, M. R.; Ziller, J. W. *Organometallics* **1986**, *5*, 25–33.
(46) Schrock, R. R.; Pedersen, S. F.; Churchill, M. R.; Ziller, J. W. *Organometallics* **1984**, *3*, 1574–1583.
(47) Stephens, F. H.; Johnson, M. J. A.; Cummins, C. C.; Kryatova, O. P.; Kryatov, S. V.; Rybak-Akimova, E. V.; McDonough, J. E.; Hoff, C. D. *J. Am. Chem. Soc.* **2005**, *127*, 15191–15200.
(48) Vaira, M. D.; Sacconi, L. *Angew. Chem., Int. Ed. Engl.* **1982**, *21*, 330–342.
(49) Di Vaira, M.; Ghilardi, C. A.; Midollini, S.; Sacconi, L. *J. Am. Chem. Soc.* **1978**, *100*, 2550–2551.
(50) Di Vaira, M.; Midollini, S.; Sacconi, L. *J. Am. Chem. Soc.* **1979**, *101*, 1757–1763.
(51) Dapporto, P.; Sacconi, L.; Stoppioni, P.; Zanobini, F. *Inorg. Chem.* **1981**, *20*, 3834–3839.
(52) Scherer, O. J.; Sitzmann, H.; Wolmershäuser, G. *J. Organomet. Chem.* **1984**, *268*, C9–C12.
(53) Scherer, O. J.; Sitzmann, H.; Wolmershäuser, G. *Angew. Chem., Int. Ed. Engl.* **1985**, *24*, 351–353.
(54) Chisholm, M. H.; Huffman, J. C.; Pasterczyk, J. W. *Inorg. Chim. Acta* **1987**, *133*, 17–18.
(55) Scherer, O. J.; Schwalb, J.; Swarowsky, H.; Wolmershäuser, G.; Kaim, W.; Gross, R. *Chem. Ber.* **1988**, *121*, 443–449.
(56) Goh, L. Y.; Chu, C. K.; Wong, R. C. S.; Hambley, T. W. *J. Chem. Soc., Dalton Trans.* **1989**, 1951–1956.
(57) Scherer, O. J.; Braun, J.; Wolmershäuser, G. *Chem. Ber.* **1990**, *123*, 471–475.
(58) Umbarkar, S.; Sekar, P.; Scheer, M. *J. Chem. Soc., Dalton Trans.* **2000**, 1135–1137.
(59) Ahlrichs, R.; Fenske, D.; Fromm, K.; Krautscheid, H.; Krautscheid, U.; Treutler, O. *Chem.−Eur. J.* **1996**, *2*, 238–244.
(60) Corey, E. J.; Cheng, X.-M. *The Logic of Chemical Synthesis*; Wiley: New York, 1995.

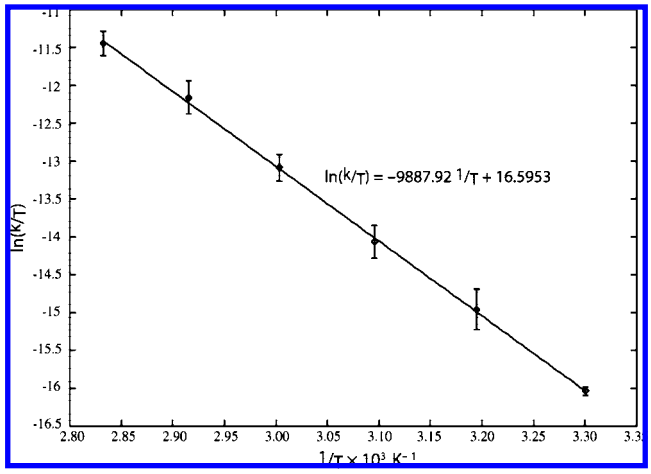

Figure 1. Eyring plot for the thermal fragmentation of **1** (error bars shown at 95% confidence interval) yielding estimated activation parameters of $\Delta H^{\ddagger} = 19.6(2)$ kcal/mol and $\Delta S^{\ddagger} = -14.2(5)$ eu.

a M≡P triple bond would provide a synthesis of these species that complements those previously explored.

Herein we report new data relevant to the mechanism of P_2 loss from the diphosphaazide complex **1** as well as on synthetically useful P_2 and $(P_2)W(CO)_5$ transfers to terminal phosphide complexes to form *cyclo*-P_3 transition-metal complexes.

Results and Discussion

Activation Parameters and Mechanism for the Thermal Fragmentation of 1. The process by which **1** is transformed into the niobium(V) imido (Mes*N)Nb(N[Np]Ar)$_3$, **2**, by loss of the P_2 fragment is unique, though it is reminiscent of reactions in which a complexed azide ligand loses N_2 and forms a metal imido.[36–38,61,62] Proulx and Bergman[36] have studied the mechanism of N_2 extrusion from the group 5 metal complexes $Cp_2(Me)Ta(N_3R)$ (Cp = C_5H_5, R = *p*-C_6H_4X) and on the basis of kinetic and Hammet analyses have proposed a mechanism for N_2 extrusion that proceeds through a four-membered metallacycle.

The kinetics of P_2 loss from **1** were monitored by ^{1}H NMR spectroscopy. Fitting the integral for the methylene resonance of **1** to a first-order decay model provided rate constants for this process over the temperature range 30−80 °C; the values ranged from $3.3(2) \times 10^{-5}$ to $3.8(6) \times 10^{-3}$ s^{-1}. The enthalpy and entropy of activation ($\Delta H^{\ddagger}$ and $\Delta S^{\ddagger}$, respectively) were estimated using Eyring analysis;[63] the data are depicted as a linear Eyring plot in Figure 1 and correspond to $\Delta H^{\ddagger} = 19.6(2)$ kcal/mol and $\Delta S^{\ddagger} = -14.2(5)$ eu. The negative sign and relatively large magnitude of $\Delta S^{\ddagger}$ indicate a highly ordered transition state and are consistent with rearrangement to the sterically congested metallacycle being the rate-limiting step to imido formation. Similar values of the activation parameters have been observed for the analogous reaction involving loss of N_2 by an η^2-complexed azide to form an imido at a sterically crowded nickel center.[62]

On the basis of these data and quantum-chemical calculations reported previously,[28] it is plausible that the mechanistic pathway for P_2 loss from complex **1** proceeds through a four-membered metallacycle intermediate. The envisioned metallacycle structure would be analogous to that of an isolated intermediate on the path to phosphaalkyne generation atop the same niobium platform.[64] The predicted mechanistic pathway is presented in Figure 2 for the model complex (2,6-^{t}Bu$_2$C$_6$H$_3$NPP)Nb(N[Me]Ph)$_3$, **1m**. The first elementary step, involving an η^2 to η^1 isomerization, was calculated to be only slightly uphill and is expected to have a small activation energy. In fact, it may be that the isomers corresponding to **1m** and **1b** are in an unobserved equilibrium in solution. Proceeding from **1b** with an inversion at N, rotation around the P−P bond, and coordination of N to the metal delivers metallacycle **1c**, the immediate precursor to P_2 elimination. This isomer was found to lie 19 kcal/mol uphill from **1m**, and its formation is likely to be rate-limiting. Though **1c** corresponds to a local energy minimum on the basis of density functional theory (DFT) calculations,[65] it is noteworthy that its energy relative to **1m** agrees well with the experimental value of $\Delta H^{\ddagger}$ and that the transition state is likely nearby. That formation of the NbPPN metallacycle **1c** rather than P_2 extrusion from **1c** is rate-limiting is supported by a comparison of $\Delta S^{\ddagger}$ for this process with that for the reaction in which ^{t}BuC≡P is generated from a preformed NbPCO metallacycle. In the latter reaction, $\Delta S^{\ddagger}$ was found to be +2 eu, consistent with a transition state in which bond breaking is causing the formation of two molecules.[63] Here we observed a negative, large-magnitude value for $\Delta S^{\ddagger}$, consistent with a reaction for which the ordering process of metallacycle formation is rate-limiting. Once the metallacycle structure is reached, the geometry is poised to eliminate the P_2 molecule into solution with concomitant formation of a strong Nb≡N imido bond.

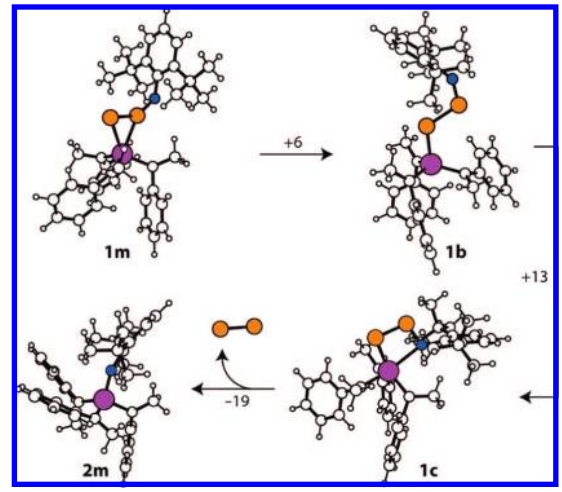

Figure 2. Pathway for P_2 elimination proposed on the basis of quantum-chemical calculations and kinetics data. The electronic energy (kcal/mol) associated with each isomerization is shown above the corresponding reaction arrow (figure adapted from ref 28).

Transfer of the P_2 Fragment from 1 to Terminal Transition-Metal Phosphide Complexes. Terminal metal phosphides appealed to us as trapping reagents for the ostensible P_2 intermediate because

(61) Cenini, S.; Gallo, E.; Caselli, A.; Ragaini, F.; Fantauzzi, S.; Pianiolino, C. *Coord. Chem. Rev.* **2006**, *250*, 1234–1253.
(62) Waterman, R. Ph.D. Thesis, University of Chicago, 2004.
(63) Anslyn, E. V.; Dougherty, D. A. *Modern Physical Organic Chemistry*; University Science Books: Sausalito, CA, 2006.
(64) Figueroa, J. S.; Cummins, C. C. *J. Am. Chem. Soc.* **2004**, *126*, 13916–13917.
(65) The large size of the model precluded the frequency calculations necessary to definitively assign these structures as local minima, though they were found to meet default convergence criteria. Analogous structures with smaller ligand sets were found to have similar geometries that were identified as energy minima with no imaginary vibrational frequencies.

Scheme 1. Transfer of P_2 to P≡M(N[^{i}Pr]Ar)$_3$ (M = Mo, W), Providing Access to the Corresponding *cyclo*-P_3 Complexes (A Mechanism Invoking the Putative P_2 Intermediate Is Shown)

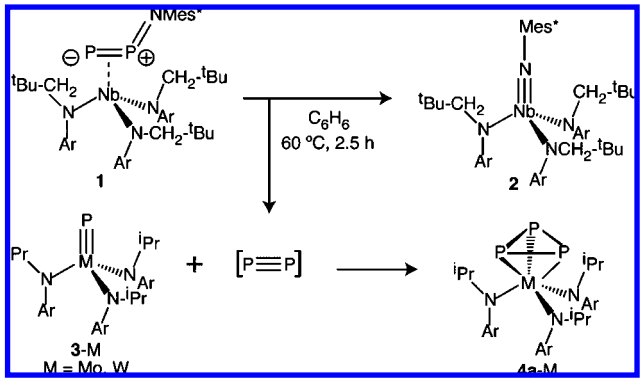

the M≡P bond has high-lying, orthogonal π orbitals and the expected products, *cyclo*-P_3 complexes, are often stable. However, terminal metal phosphides remain rare, with well-characterized examples reported only for the metals W, Mo, and Nb.[66–73] Of these, both a terminal phosphide and a *cyclo*-P_3 complex with the same ancillary ligands exist only for one system, namely, the terminal phosphide P≡Mo(N[^{i}Pr]Ar)$_3$, **3**-Mo, and its related *cyclo*-P_3 complex (P_3)Mo(N[^{i}Pr]Ar)$_3$, **4a**-Mo.[47,70] The specific supporting ligands with which the latter two molecules are decorated, while bulky enough to support a terminal phosphide complex, provide steric accessibility that allows for the formation of the pseudo-octahedral *cyclo*-P_3 complex. As a reaction partner for P_2, **3**-Mo thus seemed ideal.

The terminal phosphide **3**-Mo showed no direct reaction with **1** at 20 °C, as judged by ^{31}P and ^{1}H NMR spectroscopy. However, when the diphosphaazide complex **1** was thermolyzed at 60 °C in the presence of 1 equiv of **3**-Mo and the reaction mixture assayed by ^{31}P and ^{1}H NMR spectroscopy, signatures attributed to the *cyclo*-P_3 complex **4a**-Mo (e.g.,^{31}P NMR, $\delta = -185$ ppm) were observed. Moreover, because of its solubility properties, **4a**-Mo could be isolated from the reaction mixture in 37% yield. This is the first reaction in which a stoichiometric amount of trapping reagent was sufficient for efficient P_2 transfer from **1** to a substrate molecule. Additionally, the rate constant for the fragmentation of **1** was measured at 50 °C in benzene-d_6 and found to be independent of the concentration of **3**-Mo, remaining constant at the same value observed in the absence of **3**-Mo [$2.5(5) \times 10^{-4}$ s^{-1}]. These data are consistent with the working hypothesis that intramolecular fragmentation of **1** is rate-determining and leads to free P_2 as a reactive transient in solution, thus making it available for trapping by suitable reagents (Scheme 1).

The efficient solution-phase transfer of P_2 from **1** to **3**-Mo suggested that this methodology would provide a rational route to previously unknown *cyclo*-P_3 complexes.[74] We found that the recently reported compound P≡W(N[^{i}Pr]Ar)$_3$, **3**-W,[72] reacts in an analogous fashion and under similar conditions yields (P_3)W(N[^{i}Pr]Ar)$_3$, **4a**-W, as judged by ^{31}P and ^{1}H NMR spectroscopy. Unfortunately, we could not efficiently separate this compound from the remaining P≡W(N[^{i}Pr]Ar)$_3$ starting material and the niobium imido coproduct **2**. The ^{31}P chemical shift for **4a**-W was located at −230 ppm, which is 50 ppm upfield of that for **4a**-Mo; this is consistent both with the better back-bonding ability of the more reducing W center and with mild spin−orbit effects.[75] Similar trends have been observed in changing M from Rh to Ir and from Pd to Pt in [(*cyclo*-P_3)M(triphos)]$^{n+}$ [$n = 0$ or 1; triphos = $H_3CC(CH_2PPh_2)_3$] complexes.[76]

Transfer of P_2 to the anionic niobium terminal phosphide [P≡Nb(N[Np]Ar)$_3$]$^-$, **3**-Nb, provided access to an anionic *cyclo*-P_3 complex. In this case, the thermal sensitivity of **3**-Nb resulted in less clean reaction mixtures, but cothermolysis of **1** and [(Et_2O)Na][**3**-Nb] at 50 °C resulted in formation of [(P_3)Nb(N[Np]Ar)$_3$]$^-$, **4a**-Nb, which was isolated from the reaction mixture in 32% yield by precipitation as the bis(12-crown-4) salt. This compound has a remarkably sharp ^{31}P resonance ($\Delta\nu_{1/2} = 10$ Hz) for a niobium-bound phosphorus, a property attributable to small s character in the Nb−P bonds and consistent with a π complexation model for the binding of the P_3 unit to the metal center[76] (though higher-order effects may be responsible[77]).

Efficient Transfer of (P_2)W(CO)$_5$ from 1-W(CO)$_5$ to Terminal Phosphide Complexes. While the prospect of the P_2 molecule as a trappable intermediate continues to be intriguing, we have found it synthetically useful to transfer the P_2 unit when it is supported by a tungsten pentacarbonyl fragment.[28] In 2003, Esterhuysen and Frenking[78] performed a theoretical study of the (P_2)W(CO)$_5$ molecule and predicted that obtaining the isomer of this complex in which the P_2 molecule is bound in an η^2 fashion should be possible: this isomer was calculated to be 7 kcal/mol more stable than the one with P_2 bound in the η^1 complexation mode. While we have not yet been able to observe this molecule, we have previously reported that the complex (OC)$_5$W(Mes*NPP)Nb(N[Np]Ar)$_3$, **1**-W(CO)$_5$, undergoes unimolecular fragmentation at 20 °C in a reaction that is thought to generate the (P_2)W(CO)$_5$ molecule and that this entity can be captured with high efficiency while maintaining the reactivity of *both* PP π bonds.[28,39] We attributed the observed higher trapping yields to (P_2)W(CO)$_5$ being a longer-lived, less promiscuous intermediate than free, unstabilized P_2. Accordingly, in the present work we investigated the reaction between the putative (P_2)W(CO)$_5$ intermediate and the M≡P triple bonds

(66) Balázs, G.; Gregoriades, L. J.; Scheer, M. *Organometallics* **2007**, *26*, 3058–3075.
(67) Laplaza, C. E.; Davis, W. M.; Cummins, C. C. *Angew. Chem., Int. Ed. Engl.* **1995**, *34*, 2042–2044.
(68) Zanetti, N. C.; Schrock, R. R.; Davis, W. M. *Angew. Chem., Int. Ed. Engl.* **1995**, *34*, 2044–2046.
(69) Scheer, M.; Müller, J.; Häser, M. *Angew. Chem., Int. Ed. Engl.* **1996**, *35*, 2492–2496.
(70) Cherry, J.-P. F.; Stephens, F. H.; Johnson, M. J. A.; Diaconescu, P. L.; Cummins, C. C. *Inorg. Chem.* **2001**, *40*, 6860–6862.
(71) Figueroa, J. S.; Cummins, C. C. *Angew. Chem., Int. Ed.* **2004**, *43*, 984–988.
(72) Fox, A. R.; Clough, C. R.; Piro, N. A.; Cummins, C. C. *Angew. Chem., Int. Ed.* **2007**, *46*, 973–976.
(73) Hirsekorn, K. F.; Veige, A. S.; Wolczanski, P. T. *J. Am. Chem. Soc.* **2006**, *128*, 2192–2193.
(74) It should be noted that under conditions similar to those that proved successful for *cyclo*-P_3 formation atop the isopropylanilide platforms, the terminal phosphide of molybdenum with the more sterically encumbering *tert*-butylanilide ligand set, P≡Mo(N[^{t}Bu]Ar)$_3$, did not yield a *cyclo*-P_3 complex. Lack of *cyclo*-P_3 complex formation in this case was attributed to prohibitive steric constraints.
(75) Kaupp, M.; Malkina, O. L.; Malkin, V. G.; Pyykkö, P. *Chem.—Eur. J.* **1998**, *4*, 118–126.
(76) Di Vaira, M.; Sacconi, L.; Stoppioni, P. *J. Organomet. Chem.* **1983**, *250*, 183–195.
(77) The high symmetry and unhindered ligand rotations possible in this complex may also be responsible for the sharp signal, and interpretation of line widths for Nb-bound ligands can be complex. See: Labinger, J. A. In *Comprehensive Organometallic Chemistry*; Wilkinson, G., Stone, F. G. A., Abel, E. W., Eds.; Pergamon Press: New York, 1982; Vol. 3, pp 707−708.
(78) Esterhuysen, C.; Frenking, G. *Chem.—Eur. J.* **2003**, *2003*, 3518–3529.

of terminal metal phosphides as a potential rational, well-defined, high-yield route to $W(CO)_5$-coordinated *cyclo*-P_3 complexes.

Fragmentation of **1**-$W(CO)_5$ in the presence of **3**-M (M = Mo, W) at 20 °C resulted in the formation of the red complexes $(OC)_5W(P_3)M(N[^iPr]Ar)_3$, **4b**-M. These complexes were isolated in 50−60% yield; the yields were limited by difficulties in separating **4b**-M from the niobium imido coproduct **2**. Use of the sodium salt of **3**-Nb as a trap made possible the synthesis of the anionic $W(CO)_5$-coordinated *cyclo*-P_3 complex $[(OC)_5W(P_3)Nb(N[Np]Ar)_3]^-$, **4b**-Nb. The solubility properties of this compound hindered its isolation, so it was converted to its bis(12-crown-4) sodium salt, which displayed limited solubility in *n*-pentane, allowing for the isolation of $[(12\text{-crown-}4)_2Na]$[**4b**-Nb] in 75% yield by precipitation from Et_2O/*n*-pentane. Using **3**-Mo as a representative case, we confirmed that the first-order rate constant for fragmentation of **1**-$W(CO)_5$ was unaffected by the presence of a terminal phosphide: the rate constant for fragmentation of **1**-$W(CO)_5$ in the presence of **3**-Mo matched that found previously for **1**-$W(CO)_5$ in the presence of either no trap, 1,3-cyclohexadiene,[28] or ethylenebis(triphenylphosphine)platinum.[39] All of these data are consistent with the interpretation that $(P_2)W(CO)_5$ is released into solution prior to being consumed by M≡P triple bonds.

At 20 °C, molecules of **4b**-M (M = Mo, W, Nb) displayed magnetically equivalent P atoms as a broadened signal in the ^{31}P NMR spectrum.[79] The presence of only one signal was attributed to rapid migration of the $W(CO)_5$ unit around the *cyclo*-P_3 ring; such behavior has been well-studied in related systems.[80,81] A variable-temperature ^{31}P NMR experiment was used to confirm this assignment, and at low temperatures, three inequivalent ^{31}P environments were observed for **4b**-W (Figure S12 in the Supporting Information).[82] The conclusion that the $W(CO)_5$ unit does not dissociate from the P_3 ring in these molecules was supported by the presence of a quartet (J_{CP} = 12 Hz) for the axial carbonyl in the ^{13}C NMR spectrum of **4b**-Mo at 20 °C.

The structure of **4b**-W was determined from an X-ray crystallographic study of a red triclinic crystal grown from an Et_2O/*n*-pentane solution. The observed molecular structure exhibits the expected geometry, with a *cyclo*-P_3 ring η^3-coordinated to the tungsten tris(anilide) platform (W1) and η^1-coordinated to the $W(CO)_5$ unit (W2). The distance from W1 to the centroid of the P_3 ring is 2.167 Å, with individual W1−P distances of 2.4648(16), 2.5158(16), and 2.5201(16) Å; the shortest W1−P distance is that to P1, which also bears the pendant $W(CO)_5$ unit. Also, the two P−P interatomic distances that include P1 [2.151(2) and 2.150(2) Å] are shorter than the one that does not [2.182(2) Å]. The shorter bonds to P1 are consistent with the fact that its four-coordinate nature causes rehybridization that results in greater s character in all of its bonds. A depiction of the structure is presented in Figure 3.[83]

The $W(CO)_5$-capped niobium phosphide anion **3**-Nb-$W(CO)_5$ retains many of the properties of the parent terminal phosphide

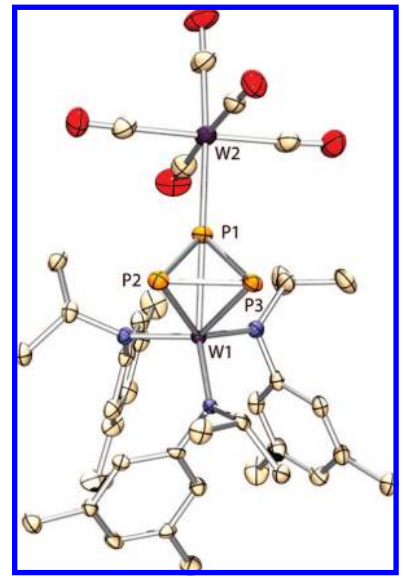

Figure 3. Structure of the $W(CO)_5$-coordinated *cyclo*-P_3 complex **4b**-W (with solvent and hydrogens omitted for clarity) drawn with thermal ellipsoids at 50% probability. See the text for values of selected metrical parameters.

Scheme 2. One-Pot Synthesis of Na[**4c**-Nb] from 2 equiv of Na[**3**-Nb-$W(CO)_5$], Invoking the $(P_2)W(CO)_5$ Molecule as an Intermediate

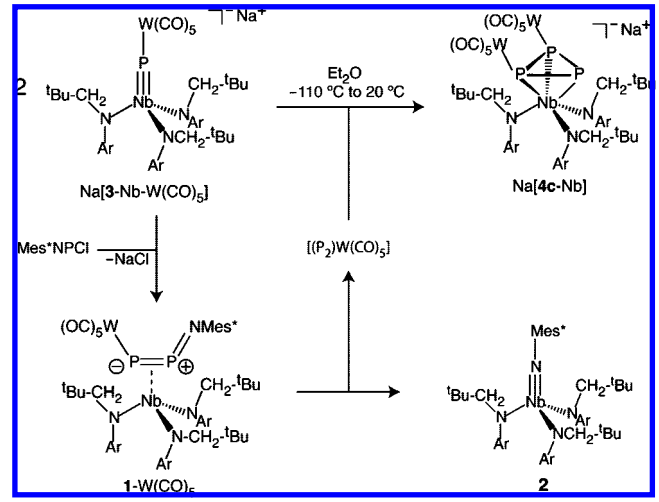

3-Nb and can act as a terminal phosphide surrogate. One example of its activity in this capacity is the role it plays in the generation of **1**-$W(CO)_5$.[28] We thus explored the ability of the Nb≡P triple bond in **3**-Nb-$W(CO)_5$ to act as a trap for the ostensible $(P_2)W(CO)_5$ intermediate in an operationally simple experiment: addition of Mes*NPCl to 2 equiv of **3**-Nb-$W(CO)_5$. The first equivalent serves to generate **1**-$W(CO)_5$, which at 20 °C releases the $(P_2)W(CO)_5$ molecule, which in turn is trapped by the second equivalent of **3**-Nb-$W(CO)_5$. As shown in Scheme 2, this generates a doubly $W(CO)_5$-coordinated, anionic *cyclo*-P_3 niobium complex **4c**-Nb, which can be isolated as its sodium salt Na[**4c**-Nb] in 80% yield following simple workup and extraction of the neutral byproduct. The ^{31}P NMR spectrum

(79) The broad nature of the NMR signal was due to the dynamic process. Variable-temperature NMR studies indicated that the ^{31}P NMR resonance became sharper as the temperature increases.

(80) Di Vaira, M.; Ehses, M. P.; Stoppioni, P.; Peruzzini, M. *Inorg. Chem.* **2000**, *39*, 2199–2205.

(81) Di Vaira, M.; Ehses, M. P.; Peruzzini, M.; Stoppioni, P. *J. Organomet. Chem.* **2000**, *593−594*, 127–134.

(82) Three ^{31}P environments are observed instead of the two expected for a C_s-symmetric $(P_3)W(CO)_5$ moiety because at low temperature, a propeller-like C_3 conformation of the anilide ligands is locked out. The combination of the C_3- and C_s-symmetric components yields a C_1-symmetric structure.

(83) Full crystallographic data (in the form of CIF files) are available from the Cambridge Crystallographic Data Centre (CCDC) under deposition numbers 661324−661326, 675339, 675340, and 680219. These data can be obtained free of charge from the CCDC via www.ccdc.cam.ac.uk/data_request/cif.

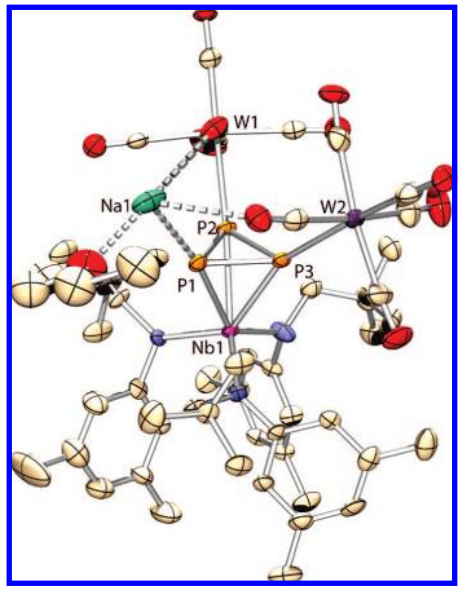

Figure 4. Structure of the *cyclo*-P_3 complex [(Et_2O)Na][**4c**-Nb] (with benzene of crystallization and hydrogens omitted for clarity) drawn with thermal ellipsoids at 50% probability. See the text for values of selected metrical parameters.

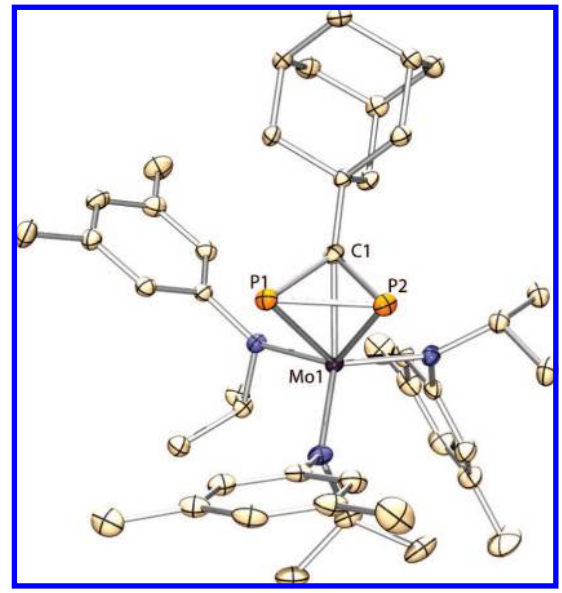

Figure 5. Structure of complex **5** (with solvent and hydrogens omitted for clarity) drawn with thermal ellipsoids at 50% probability. See the text for values of selected metrical parameters.

again shows a single broad resonance indicating dynamic behavior of the $W(CO)_5$ units.[79]

The structure of [(Et_2O)Na][**4c**-Nb] was determined from an X-ray crystallographic study of a red-orange triclinic crystal grown from benzene at 22 °C in the presence of trace Et_2O. The solid-state structure shows the expected geometry for the NbP_3 core, with a closely associated sodium cation. The coordination sphere of the sodium ion is made up of the uncapped phosphorus (P1) of the *cyclo*-P_3 unit, two intramolecular carbonyl oxygen contacts, one carbonyl oxygen contact from each of two neighboring molecules, and the oxygen of Et_2O. This coordination results in an extended 1D chain that runs through the crystal, with benzene molecules of crystallization filling voids in the lattice (Figure S23 in the Supporting Information). The distance from Nb1 to the centroid of the P_3 ring is 2.278 Å, and the individual Nb1−P distances vary from 2.560(2) to 2.665(2) Å. The P−P interatomic distances around the ring vary from 2.164(2) to 2.188(2) Å, and the sodium ion resides at a distance of 3.026(4) Å from P1. The structure of the anionic core with an included sodium ion is presented in Figure 4.[83]

Phosphaalkyne Addition to a Terminal Phosphide Complex. In the previous sections, triply bonded P_2 has been invoked as a likely intermediate in reactions forming *cyclo*-P_3 complexes. To model this process, we sought an example of a reaction in which a terminal phosphide complex would be seen to combine with an established and directly observable phosphorus triple-bond system.

Phosphorus has been dubbed a "carbon copy" because of similarities in the reactivity of RC and P units.[84] Thus, a phosphaalkyne could serve in the role of P_2 as a reaction partner for a metal terminal phosphide to yield a *cyclo*-CP_2 complex. In 1985, Becker et al.[85] reported evidence for the reaction between ^{t}BuCP and in situ generated $(^t$BuO$)_3$W≡P, and this work was followed up by Scheer and co-workers.[86]In these reactions, the cycloaddition products have further reacted via 1,3-OR migration to yield the diphosphametallacyclobutadiene complexes $(^t$BuO$)P_2C(R)W(O^t$Bu$)_2$. Phosphaalkynes are also reported to combine with the transient phosphide complex

Scheme 3. Combination of Mo≡P and C≡P Triple Bonds To Yield a *cyclo*-CP_2 Complex

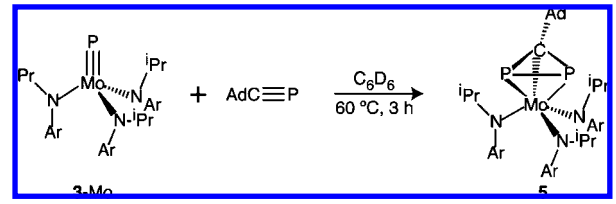

$Cp^*(CO)_2W{\equiv}PW(CO)_5$ to yield products that rapidly undergo subsequent transformations.[87,88]

Reaction of **3**-Mo and AdC≡P (Ad = 1-adamantyl) over the course of 3 h at 60 °C in C_6D_6 gave a new compound with a ^{31}P NMR signal at −249 ppm as the major product. This upfield chemical shift compares well to that of the *cyclo*-P_3 complex **4a**-Mo and is consistent with the formation of $(AdCP_2)Mo(N[^i$Pr]Ar$)_3$, **5** (Scheme 3). Also present in the reaction mixture was a minor product displaying a pair of doublet ^{31}P resonances at −121 and +571 ppm (J_{PP} = 450 Hz). These signals are consistent with a ligand-migration product analogous to those of Becker et al.[85] and Scheer and co-workers,[86] namely, the complex $(Ar[^i$Pr]N$)P_2C$-$(Ad)Mo(N[^i$Pr]Ar$)_2$.

The product **5** was crystallized from toluene/*n*-pentane at −35 °C, and an X-ray diffraction study confirmed the formation of the *cyclo*-CP_2 complex (Figure 5).[83] The Mo1−P1 and Mo1−P2 distances are 2.4838(8) and 2.4691(7) Å, respectively, while C1 lies 2.1830(19) Å from the metal. The P1−C1 and P2−C1 distances are 1.798(2) and 1.810(2) Å, respectively, and the P1−P2 distance is 2.1374(9) Å. The relatively short P−P

(84) Dillon, K. B.; Mathey, F.; Nixon, J. F. *Phosphorus: The Carbon Copy*; Wiley: Chichester, U.K., 1998.
(85) Becker, G.; Becker, W.; Knebl, R.; Schmidt, H.; Weeber, U.; Westerhausen, M. *Nova Acta Leopold.* **1985**, *59*, 55–67.
(86) Scheer, M.; Kramkowski, P.; Schuster, K. *Organometallics* **1999**, *18*, 2874–2883.
(87) Scheer, M.; Himmel, D.; Johnson, B. P.; Kuntz, C.; Schiffer, M. *Angew. Chem., Int. Ed.* **2007**, *46*, 3971–3975.
(88) Scheer, M.; Leiner, E.; Kramkowski, P.; Schiffer, M.; Baum, G. *Chem.—Eur. J.* **1998**, *4*, 1917–1923.

distance can be attributed to the geometric constraints that result from having a carbon atom in the three-membered ring. The formation of this product provides clear evidence that terminal phosphide complexes react with phosphorus triple bonds, leading to smooth formation of the corresponding metallatetrahedranes.

Mechanism and Energetics of *cyclo*-P_3 Formation. The formation of a *cyclo*-P_3 complex from the ostensible reaction of a P≡P triple bond with a M≡P triple bond contrasts with the analogous organometallic reaction, where a metallacyclobutadiene complex, the intermediate in alkyne metathesis reactions, is often observed.[40–42] Interestingly, Schrock and co-workers[43,44] have shown that introduction of a base to certain metallacyclobutadiene complexes can cause their isomerization to cyclopropenyl complexes. The direct formation of a *cyclo*-P_3 complex could proceed in concerted fashion along an idealized C_s reaction coordinate with orthogonal approach of the two triple bonds, though such a process would be forbidden by orbital symmetry. Alternatively, a lower-energy pathway may exist wherein a triphosphametallacyclobutadiene intermediate is formed through a more facile suprafacial [2 + 2] cycloaddition; this route would be symmetry-allowed because of the presence of d orbitals in the bonding. This latter reaction could then be followed by a rapid intramolecular isomerization to yield the transition-metal *cyclo*-P_3 complex. These two pathways have been considered computationally for the analogous organometallic reaction, and one such study predicted the suprafacial [2 + 2] addition to be the lower-energy route.[89] Mechanisms for the interconversion of the two isomers have also been considered on a variety of metal platforms for the organometallic analogue and may operate similarly here.[90] The relative thermodynamic stabilities of metallacyclobutadiene and metallatetrahedrane (cyclopropenyl) complexes have also been studied, but the phosphorus analogues have been negelected.[91,92] Notably, Stephan and co-workers[93–94] have reported what is to our knowledge the only example of a triphosphacyclobutadiene metal complex, the anionic species $[Cp^*_2Zr(\kappa^2\text{-}P_3)]^-$, while *cyclo*-$P_3$ complexes are far more common (see above).[95]

Quantum-chemical calculations on isomers of the model complex $(P_3)Mo(N[Me]Ph)_3$ were performed in order to better understand the relative energies of the two isomers and the reactants. The optimized geometries are shown in Figure 6, and the energies of the *cyclo*-P_3 and triphosphametallacyclobutadiene isomers relative to free P_2 and the terminal metal phosphide are given in Table 1. The optimized geometry of the metallacyclic isomer displays a distorted square-pyramidal geometry at the metal and a planar triphosphametallacyclobutadiene ring having interatomic distances consistent with alternating single and double bonds. The optimized distances are as follows: Mo1−P1, 2.254 Å; P1−P2, 2.211 Å; P2−P3, 2.030 Å; and P3−Mo1, 2.542 Å. It is easy to envisage how this structure might result from in-plane approach of the P2−P3 and Mo1−P1

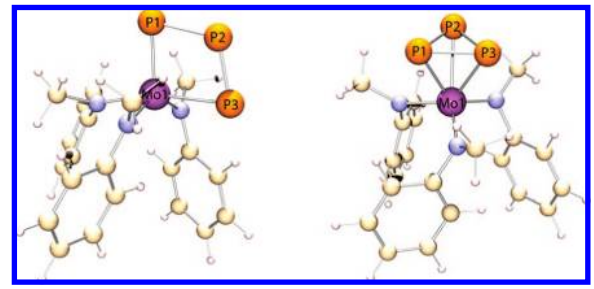

Figure 6. DFT-optimized geometries for two isomers of the model compound $(P_3)Mo(N[Me]Ph)_3$: (left) $(\kappa^2\text{-}P_3)Mo(N[Me]Ph)_3$; (right) (*cyclo*-$P_3$)$Mo(N[Me]Ph)_3$.

Table 1. Relative Electronic Energies of Model Species Related to the Reaction **3**-Mo + P_2 → **4a**-Mo

isomer	relative energy (kcal/mol)
P≡Mo(N[Me]Ph)$_3$ + P_2	0
(κ^2-P_3)Mo(N[Me]Ph)$_3$	–10.7
(*cyclo*-P_3)Mo(N[Me]Ph)$_3$	–39.5

vectors. In fact, this structure is quite reminiscent of those calculated by Zeigler and co-workers[89] for the analogous organometallic reaction, with the exception that the bond-length alternation seen here was not present in the minimum-energy structure but instead was seen along the reaction pathway.

On the basis of these geometries and energies and the same orbital-symmetry arguments that hold for the organometallic system, it is tempting to suggest that triphosphacyclobutadienes are formed as intermediates in the capture of solution-phase P_2. This process would then be followed by rearrangement at the metal to form the *cyclo*-P_3 complex, accompanied by the release of 30 kcal/mol of energy. However, we cannot rule out direct formation of the *cyclo*-P_3 complex via perpendicular approach of P_2 to the M≡P bond, and despite the higher barrier expected for this latter reaction, it may be the preferred pathway for certain systems.[89]

Functionalizations of Anionic *cyclo*-P_3 Complexes. Functionalizations of *cyclo*-P_3 complexes were first reported for the series $(P_3)M(triphos)$ (M = Co, Rh, Ir) and required the highly electrophilic reagents $[Me_3O][BF_4]$ or MeOTf to afford the methylated species.[96] The $[Me(P_3)Co(triphos)]^+$ complex shows structural distortions similar to those in **4b**-W, where rehybridization at the methylated phosphorus results in a shortening of bonds to this atom, but no major structural changes are detected. The anionic nature of the *cyclo*-P_3 niobium complexes described herein gives them greater nucleophilic character, allowing functionalization using milder reagents to give a variety of products (Chart 1).

Treating [(12-crown-4)$_2$Na][**4b**-Nb] with triphenyltin chloride and heating the reaction mixture to 75 °C for 14 h affords the P-stannylated species $(OC)_5W(Ph_3SnP_3)Nb(N[Np]Ar)_3$, **6**. The ^{31}P NMR spectrum contained a multiplet ($\delta = -196$ ppm) for the stannylated phosphorus and a very broad resonance ($\delta = -235$ ppm) for the $(P_2)W(CO)_5$ unit, indicative of $W(CO)_5$ mobility across an incompletely reduced P−P π bond. X-ray crystallographic structure determination provided data consistent with the assignment of the new ligand as an η^2-triphosphirene coordinated to the niobium tris(anilide) platform (Figure 7). This is reflected in the two short Nb−P distances [2.5611(9) and 2.5676(9) Å] and one long interaction [2.8379(9) Å]. The P1−P2 distance of 2.156(1) Å, which is intermediate between the lengths of double (2.00−2.04 Å)^2 and single (cf. 2.21 Å in

(89) Woo, T.; Folga, E.; Ziegler, T. *Organometallics* **1993**, *12*, 1289–1298.
(90) Jemmis, E. D.; Hoffmann, R. *J. Am. Chem. Soc.* **1980**, *102*, 2570–2575.
(91) Anslyn, E. V.; Bursich, M. J.; Goddard, W. A. I. *Organometallics* **1988**, *7*, 98–105.
(92) Lin, Z.; Hall, M. B. *Organometallics* **1994**, *13*, 2878–2884.
(93) Fermin, M. C.; Ho, J. W.; Stephan, D. W. *J. Am. Chem. Soc.* **1994**, *116*, 6033–6034.
(94) Fermin, M. C.; Ho, J. W.; Stephan, D. W. *Organometallics* **1995**, *14*, 4247–4256.
(95) Witmore, K. H. In *Advances in Organometallic Chemistry*; Stone, F. G. A., West, R., Eds.; Academic Press: San Diego, 1998; Vol. 42.

Chart 1. *cyclo*-P_3 and η^2-Triphosphirene Complexes Derived via Ostensible P_2-Trapping Reactions

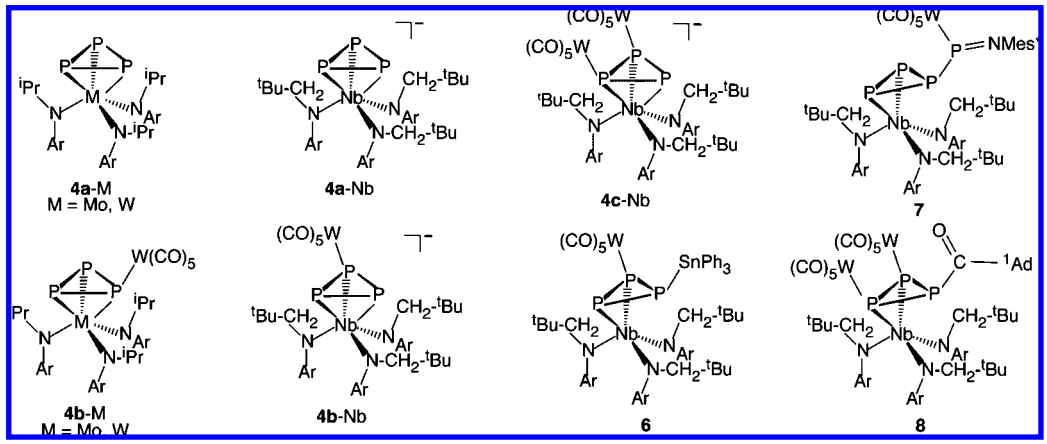

P_4) P−P bonds, is similarly consistent with a coordinated diphosphene model, while the P1−P3 and P2−P3 bonds are longer [2.188(1) and 2.213(1) Å, respectively]. The P3−Sn1 distance is 2.5288(9) Å.[83,97] The η^2-triphosphirene moiety has a precedent in the P_4-derived triphosphirene complexes reported by Peruzzini and co-workers.[98,99]

The reactions of more unusual electrophiles with **4c**-Nb were also examined in order to explore the limits of functionalized triphosphirene complexes. The complex **4c**-Nb was found to react readily with Mes*NPCl. Analysis of the reaction mixture at early stages using ^{31}P NMR spectroscopy revealed a mixture of products. After the reaction mixture was allowed to stand for 12 h, the product distribution converged onto a single product, **7**. This final product exhibited a downfield quartet (δ 367, J_{PP} = 105 Hz) and an upfield doublet (δ −137, J_{PP} = 105 Hz) in the ^{31}P NMR spectrum (Figure 8). The product had been expected to contain a Mes*NP-P(PW(CO)$_5$)$_2$ unit that would show a downfield doublet of triplets (for the iminophosphane phosphorus) as well as a doublet of doublets and a doublet of triplets upfield (for the two types of P atoms in the *cyclo*-P_3 ring). The observed quartet was particularly interesting because it suggested a Mes*NP$^+$ unit possessing equivalent interactions with *all three* P atoms of the *cyclo*-P_3 moiety.

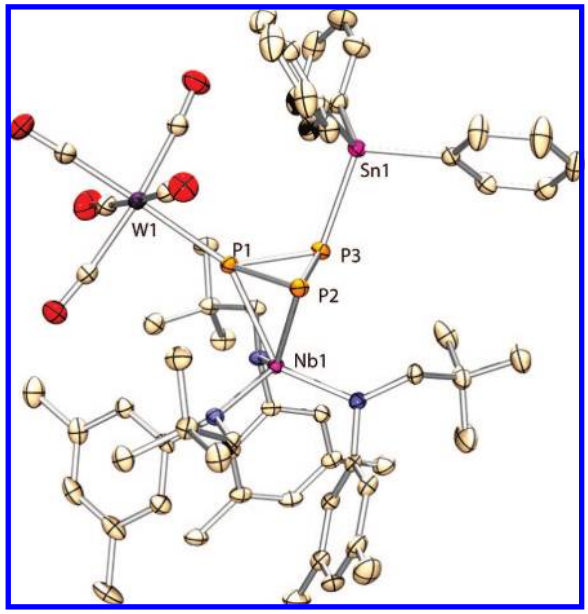

Figure 7. Structure of the stannyltriphosphirene complex **6** (with solvent and hydrogens omitted for clarity) drawn with thermal ellipsoids at 50% probability. See the text for values of selected metrical parameters.

X-ray crystallographic structure determination of **7** again revealed an η^2-triphosphirene structure, analogous to that of the stannyl derivative **6**. In the structure of **7**, however, one W(CO)$_5$ unit has migrated to the iminophosphane phosphorus and the second W(CO)$_5$ of the starting material has been lost (Figure 9). The P−P distance between the Mes*NP unit and the *cyclo*-P_3 moiety is 2.2326(11) Å, while that in the coordinated diphosphene is 2.1650(11) Å; the other two P−P distances are 2.20 Å. The two Nb−P distances involving the diphosphene unit are 2.5655(9) and 2.5988(8) Å, and that for the P atom bearing the Mes*NP$^+$ unit is 3.0194(8) Å.[83] Here the Mes*NP$^+$ group demonstrates its ambiphilic character: it acts as a Lewis acid toward the *cyclo*-P_3 donor and as a Lewis base toward the W(CO)$_5$ unit.[100,101]

The ^{31}P NMR spectrum of this product can be explained in terms of a room-temperature dynamic process whereby the Mes*NP unit migrates around the *cyclo*-P_3 ring by means of formation and release of Nb−P interactions. Cooling to −70 °C slowed these processes, and the ^{31}P NMR spectrum at this temperature showed the expected four inequivalent phosphorus nuclei (Figure S18 in the Supporting Information). Migration of RNP (R = Mes*, ^{i}Pr$_3$Si, ^{t}Bu) units around unsaturated rings has been observed previously in RNPCp*.[102,103] Interestingly, the solid-state structure of ^{i}Pr$_3$SiNPCp* exhibits a "slipped" geometry wherein the C−C bond of the Cp* ring binds in an η^2 fashion to the P atom. It is also noteworthy that the RNP unit is not unique in this behavior: the diphosphene Cp*P=PCp* exhibits a single methyl environment even at temperatures as low as −80 °C.[104]

(96) Capozzi, G.; Chiti, L.; Di Vaira, M.; Peruzzini, M.; Stoppioni, P. *J. Chem. Soc., Chem. Commun.* **1986**, 1799–1800.
(97) This same product **6** could be isolated in small quantities by selective crystallization from the reaction between **4c**-Nb and Ph_3SnCl via a reaction where loss of W(CO)$_5$ occurs.
(98) Barbaro, P.; Ienco, A.; Mealli, C.; Peruzzini, M.; Scherer, O.; Schmitt, G.; Vizza, F.; Wolmershäuser, G. *Chem.—Eur. J.* **2003**, *9*, 5195–5210.
(99) Yakhvarov, D.; Babaro, P.; Gonsalvi, L.; Carpio, S. M.; Midollini, S.; Orlandini, A.; Peruzzini, M.; Sinyashin, O.; Zanobini, F. *Angew. Chem., Int. Ed.* **2006**, *45*, 4182–4185.
(100) Gudat, D. *Coord. Chem. Rev.* **1997**, *163*, 71–106.
(101) Burford, N.; Cameron, T. S.; LeBlanc, D. J.; Losier, P.; Sereda, S.; Wu, G. *Organometallics* **1997**, *16*, 4712–4717.
(102) Gudat, D.; Schiffner, H. M.; Nieger, M.; Stalke, D.; Blake, A. J.; Grondey, H.; Niecke, E. *J. Am. Chem. Soc.* **1992**, *114*, 8857–8862.
(103) Gudat, D.; Niecke, E.; Krebs, B.; Dartmann, M. *Organometallics* **1986**, *5*, 2376–2377.

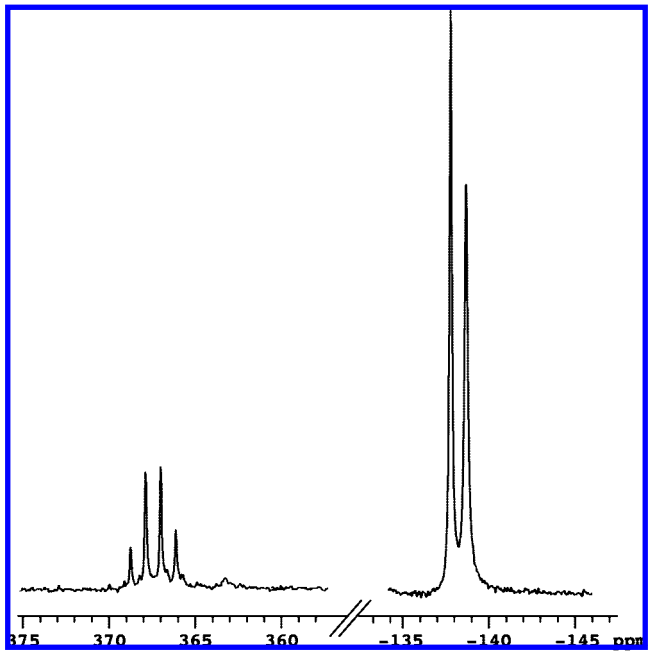

Figure 8. ^{31}P NMR spectrum (20 °C, C_6D_6, 121 MHz) of **7**, showing only an upfield doublet and a downfield quartet despite the presence of four inequivalent phosphorus centers in the solid-state structure.

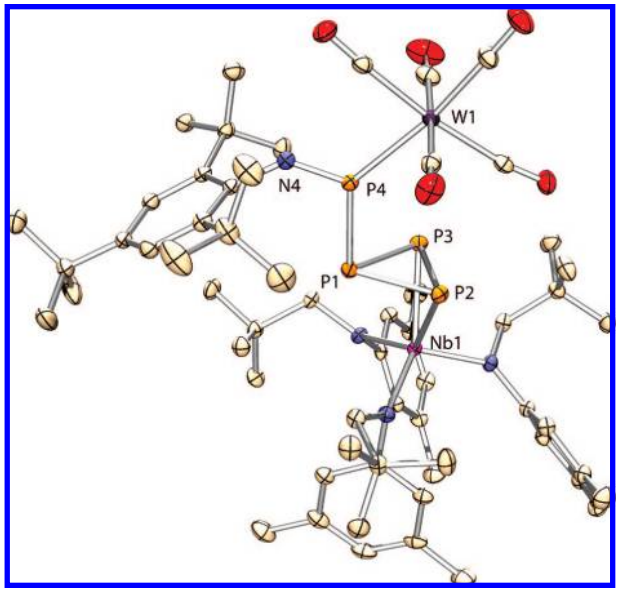

Figure 9. Structure of complex **7** (with solvent and hydrogens omitted for clarity) drawn with thermal ellipsoids at 50% probability. See the text for values of selected metrical parameters.

As an avenue to the use of *cyclo*-P_3 complexes as P_3 transfer reagents, we synthesized a P-acylated triphosphirene complex via the reaction between the sodium salt of **4c**-Nb and 1-adamantylcarbonyl chloride in thawing Et_2O followed by brief warming to room temperature and rapid workup. Analysis of the reaction mixture following removal of NaCl using ^{31}P NMR spectroscopy revealed the expected broad resonance attributed to the coordinated diphosphene and a sharp triplet for the acylated P center; the ^{1}H NMR spectrum revealed one new C_s-symmetric species. This red complex, $\{(OC)_5W\}_2AdC(O)P_3$-$Nb(N[Np]Ar)_3$, **8**, was isolated in 60% yield by precipitation from Et_2O at −35 °C. A red crystal grown at this temperature in Et_2O was subjected to X-ray diffraction analysis, which revealed the predicted η^2-bound triphosphirene (Figure 10). In **8,** the diphosphene P−P distance is 2.1453(9), and the other P−P distances are 2.2008(9) and 2.2320(9) Å. The Nb−P distances are 2.5770(7) and 2.6122(7) Å to the diphosphene unit and 3.0292(7) Å to the P atom bearing the acyl unit.[83]

Complex **8** is thermally unstable and decomposes at 20 °C with precipitation of a red microcrystalline material and formation of $ONb(N[Np]Ar)_3$ as the principal benzene- and THF-soluble product. The red precipitate is thought to be composed of compounds of the formula $[\{(OC)_5W\}_2P_3CAd]_n$ but could not be definitively identified because of its poor solubility properties. Further efforts to understand this P_3 transfer reaction are in progress.

Conclusions

This work has demonstrated the successful use of M≡P triple bonds as a class of reaction partners in the transfer of the P_2-containing fragments in **1** and **1**-$W(CO)_5$. The first-order kinetics observed in the presence or absence of the P_2-accepting substrate are consistent with the working hypothesis that P_2 and $(P_2)W(CO)_5$ are present in solution as reactive intermediates following the fragmentation of **1** and **1**-$W(CO)_5$, respectively. Reactions between in situ generated P_2 and transition-metal phosphide complexes thus provide a general, rational synthesis of *cyclo*-P_3 complexes. A *cyclo*-CP_2 complex was also synthesized by the combination of a M≡P triple bond with the C≡P triple bond of a phosphaalkyne. The reactivities demonstrated herein are the first examples of "side-on" reactivity for the terminal phosphide complexes **3**-M (M = Mo, W, Nb).[66] Furthermore, functionalizations of the anionic *cyclo*-P_3 compounds **4b**- and **4c**-Nb have set the stage for exploration of these complexes as P_3 transfer reagents.

Experimental Section

General Considerations. All of the manipulations were performed in a Vacuum Atmospheres model MO-40 M glovebox under an atmosphere of purified N_2. Anhydrous grade, oxygen-free tetrahydrofuran (THF) was purchased from Aldrich and further dried by passage through a column of molecular sieves and stirring with sodium for at least 12 h prior to filtration through Celite to remove sodium. Dimethoxyethane was distilled off sodium metal and filtered through activated alumina prior to use. Hexamethyldisiloxane $[O(SiMe_3)_2]$ was vacuum-transferred off sodium benzophenone and stored over molecular sieves. All of the other solvents were made anhydrous and oxygen-free by bubble degassing using N_2 and purification through columns of alumina and Q5.[105] Deuterated solvents for NMR spectroscopy were purchased from Cambridge Isotope Laboratories. Benzene-d_6 and toluene-d_8 were degassed and stored over molecular sieves for at least 2 days prior to use. Pyridine-d_5 was distilled off sodium and stored over molecular sieves. Celite 435 (EM Science), 4 Å molecular sieves (Aldrich), and alumina (EM Science) were dried by heating at 200 °C under dynamic vacuum for at least 24 h prior to use. The compounds $[(Et_2O)Na][P{\equiv}Nb(N[Np]Ar)_3]$,[71] $[(Et_2O)Na][(OC)_5WP{\equiv}Nb(N[Np]Ar)_3]$,[28] (Mes*NPP)$Nb(N[Np]Ar)_3$[28] Mes*NPCl,[106]

(104) Jutzi, P.; Meyer, U.; Krebs, B.; Dartmann, M. *Angew. Chem., Int. Ed. Engl.* **1986**, *25*, 919–921.
(105) Pangborn, A. B.; Giardello, M. A.; Grubbs, R. H.; Rosen, R. K.; Timmers, F. J. *Organometallics* **1996**, *15*, 1518–1520.
(106) Niecke, E.; Nieger, M.; Reichert, F. *Angew. Chem., Int. Ed. Engl.* **1988**, *27*, 1715.
(107) Williams, T.; Kelley, C. Gnuplot, 2002; http://www.gnuplot.info.
(108) Sheldrick, G. M. SHELXTL, Bruker AXS: Madison, WI, 2005.
(109) Sheldrick, G. M. *Acta Crystallogr.* **1990**, *A46*, 467–473.

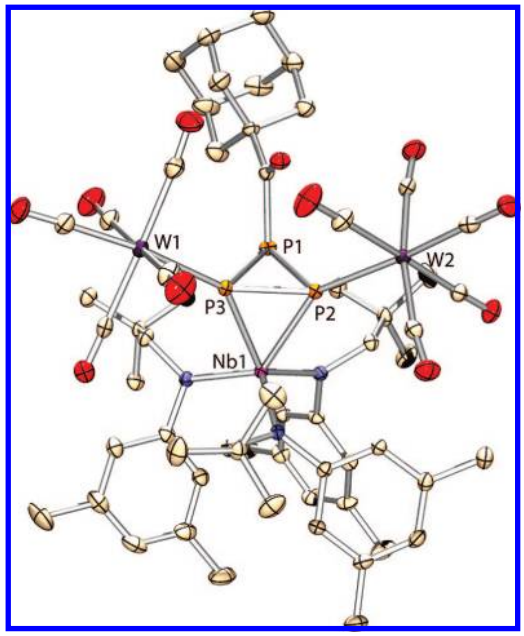

Figure 10. Structure of complex **8** (with solvent and hydrogens omitted for clarity) drawn with thermal ellipsoids at 50% probability. See the text for values of selected metrical parameters.

P≡Mo(N[^{t}Pr]Ar)$_3$,[70] and P≡W(N[^{t}Pr]Ar)$_3$[72] were prepared according to literature procedures. AdC≡P was purchased from Fluka and used as received. All of the glassware was oven-dried at temperatures above 170 °C prior to use. NMR spectra were obtained on Varian Mercury 300 or Varian Inova 500 instruments equipped with Oxford Instruments superconducting magnets and referenced to residual C_6D_5H (7.16 ppm), $CHCl_3$ (7.27 ppm), $CD_3C_6D_4H$ (7.00 ppm), or C_5D_4HN (8.74 ppm). ^{13}C NMR spectra were referenced to solvent resonances, and ^{31}P NMR spectra were referenced externally to 85% H_3PO_4 (0 ppm). Elemental analyses were performed by Midwest Microlab, LLC (Indianapolis, IN).

[(12-crown-4)$_2$Na][(P$_3$)Nb(N[Np]Ar)$_3$]. Solid (Mes*NPP)Nb(N[Np]Ar)$_3$ (405 mg, 0.41 mmol, 1 equiv) and [(Et$_2$O)Na][P≡Nb(N[Np]Ar)$_3$] (325 mg, 0.41 mmol, 1 equiv) were mixed and dissolved in benzene (5 g). The resulting red solution was sealed in a Teflon-stoppered tube and heated to 55 °C for 2.5 h. The resulting dark-orange solution was then dried in vacuo and dissolved in *n*-pentane (~5 mL). To this solution was added 12-crown-4 (150 mg, 0.85 mmol, 2.1 equiv) as an Et$_2$O solution (3 mL). A precipitate formed, and the solution was allowed to stir for 15 min. After this time, the suspension was concentrated to dryness in vacuo, and the residue was dissolved in THF (2.5 mL); the resulting solution was filtered through a plug of Celite. The filtered solution was layered with Et$_2$O (2 mL) and *n*-pentane (3 mL) and then cooled to −35 °C for several days. The resulting orange powder was collected on a sintered glass frit, washed with *n*-pentane, and dried in vacuo (135 mg, 0.12 mmol, 30% yield). $^{31}P\{^1H\}$ NMR (C_6D_5N, 20 °C, 121.5 MHz): δ −183 (s, $\Delta\nu_{1/2}$ = 10 Hz) ppm. ^1H NMR (C_5D_5N, 20 °C, 500 MHz): δ 7.01 (s, 6H, *o*-Ar), 6.61 (s, 3H, *p*-Ar), 4.22 (s, 6H, N−CH_2), 3.59 (s, 32H, crown), 2.35 (s, 18H, Ar−CH_3), 1.13 (s, 27H, ^{t}Bu) ppm. $^{13}C\{^1H\}$ NMR (C_5D_5N, 20 °C, 125.8 MHz): δ 160.2 (*ipso*-Ar), 137.1 (*o*-Ar), 124.5 (*m*-Ar), 122.9 (*p*-Ar), 71.9 (N−*C*H$_2$), 67.1 (crown), 36.5 (*C*(CH$_3$)$_3$), 30.5 (C(*C*H$_3$)$_3$), 22.4 (Ar−*C*H$_3$) ppm. Anal. Calcd for $C_{60}H_{92}N_3O_{13}P_3NaNbW$: C, 58.35; H, 8.19; N, 3.71. Found: C, 58.03; H, 8.24; N, 3.73.

[(12-crown-4)$_2$Na][(OC)$_5$W(P$_3$)Nb(N[Np]Ar)$_3$]. To a thawing Et$_2$O solution (7 mL) of [(Et$_2$O)Na][(OC)$_5$WP≡Nb(N[Np]Ar)$_3$] (304 mg, 0.27 mmol,) was added dropwise a thawing Et$_2$O solution (3 mL) of Mes*NPCl (88 mg, 0.27 mmol, 1.0 equiv), affording a color change to deep-red. The reaction mixture was allowed to stir for 1 min, and then a 22 °C solution of [(Et$_2$O)Na][P≡Nb(N[Np]Ar)$_3$] (233 mg, 0.29 mmol, 1.1 equiv) in Et$_2$O (4 mL) was added. The resulting solution was stirred for 3 h at 22 °C and remained red during this time. The reaction mixture was then filtered through a bed of Celite to remove salts, and the filtrate was concentrated to dryness in vacuo. The resulting red powder was dissolved in hexane (10 mL) and dried once more. A solution of the residue in 1:1 benzene/*n*-pentane (10 mL) was prepared, and to it was added a solution of 12-crown-4 (160 mg, 0.91 mmol, 3.3 eq) in Et$_2$O (2 mL). After the solution was stirred for 5 min, it was evaporated to dryness and the resulting powder slurried in *n*-pentane/Et$_2$O (15 mL/5 mL). A light-orange powder (265 mg) was collected atop a sintered glass frit, and the dark red filtrate was dried in vacuo. The resulting residue was dissolved in *n*-pentane/THF (20 mL total) and stored at −35 °C to precipitate another crop of orange powder, which was collected on a frit and washed with *n*-pentane. The combined orange solids were dried in vacuo to constant mass (295 mg, 0.203 mmol, 75% yield). $^{31}P\{^1H\}$ NMR (C_6D_5N, 50 °C, 202.5 MHz): δ −203 (br s, $\Delta\nu_{1/2}$ = 520 Hz) ppm. ^1H NMR (C_5D_5N, 20 °C, 500 MHz): δ 6.74 (s, 6H, *o*-Ar), 6.69 (s, 3H, *p*-Ar), 4.18 (br s, 6H, N−CH_2), 3.58 (s, 32H, crown), 2.30 (s, 18H, Ar−CH_3), 1.04 (s, 27H, ^{t}Bu) ppm. $^{13}C\{^1H\}$ NMR (C_5D_5N, 20 °C, 125.8 MHz): δ 203.8 (br, *ax*-*C*O), 201.7 (J_{CW} = 126 Hz, *eq*-*C*O), 157.7 (*ipso*-Ar), 137.5 (*o*-Ar), 124.9 (*m*-Ar), 124.6 (*p*-Ar), 73.2 (br, N−*C*H$_2$), 66.2 (crown), 36.7 (*C*(CH$_3$)$_3$), 30.4 (C(*C*H$_3$)$_3$), 22.2 (Ar−*C*H$_3$) ppm. IR (thin film, KBr) ν: 2917 (m), 2051 (s), 1917 (vs), 1874 (s), 1602 (m), 1098 (s) cm^{-1}. Anal. Calcd for $C_{60}H_{92}N_3O_{13}P_3NaNbW$: C, 49.49; H, 6.37; N, 2.89. Found: C, 49.44; H, 6.63; N, 3.05.

Na[{(OC)$_5$W}$_2$(P$_3$)Nb(N[Np]Ar)$_3$]. To a thawing Et$_2$O solution (100 mL) of [(THF)$_3$Na][(OC)$_5$WP≡Nb(N[Np]Ar)$_3$] (3.0 g, 2.38 mmol, 2.0 equiv) was added dropwise a thawing Et$_2$O solution (12 mL) of Mes*NPCl (390 mg, 1.19 mmol, 1.0 equiv). This solution was stirred for 4 h at 22 °C, after which the reaction mixture was filtered through a bed of Celite and the filtrate concentrated to dryness in vacuo. To the resulting red powder was added Et$_2$O, forming a red solution that contained some undissolved yellow solids (the niobium imido **2**). The solution was then filtered through Celite, and the yellow solids were washed with minimal Et$_2$O until the washings were no longer red. The yellow solids were discarded, and the red filtrate was dried in vacuo to give a red powder that was slurried in hexane/benzene (10 mL each) before the mixture was stripped to dryness once more. The resulting solids were slurried in hexane/benzene (25 mL/10 mL), and the suspended fine red powder was collected atop a sintered glass frit, washed with *n*-pentane until the washings were colorless, and then dried in vacuo (1.41 g, 0.99 mmol, 83% yield). $^{31}P\{^1H\}$ NMR (C_5D_5N, 20 °C, 202.5 MHz): δ −216 (br s, $\Delta\nu_{1/2}$ = 120 Hz) ppm. ^1H NMR (C_5D_5N, 20 °C, 500 MHz): δ 6.83 (s, 6H, *o*-Ar), 6.73 (s, 3H, *p*-Ar), 4.11 (s, 6H, N−CH_2), 2.36 (s, 18H, Ar−CH_3), 0.97 (s, 27H, ^{t}Bu) ppm. $^{13}C\{^1H\}$ NMR (C_5D_5N, 20 °C, 125.8 MHz): δ 202.3 (m, *ax*-*C*O), 199.9 (J_{CW} = 126 Hz, *eq*-*C*O), 156.3 (*ipso*-Ar), 137.7 (*o*-Ar), 125.8 (*m*-Ar), 124.6 (*p*-Ar), 72.2 (br, N−*C*H$_2$), 36.5 (*C*(CH$_3$)$_3$), 30.3 (C(*C*H$_3$)$_3$), 22.1 (Ar−*C*H$_3$) ppm. IR (*Et$_2$O*, KBr) ν : 2089 (s), 2066 (s), 2060 (s), 1984 (s), 1975 (s), 1949 (vs), 1921 (vs), 1898 (vs), 1803 (s), 1602 (m), 1586 (m) cm^{-1}. Anal. Calcd for $C_{49}H_{60}$-

(110) Sheldrick, G. *Acta Crystallogr.* **2008**, *A64*, 112–122.
(111) Sheldrick, G. M. SHELXL-97: Program for Crystal Structure Determination; University of Göttingen: Göttingen, Germany, 1997.
(112) te Velde, G.; Bickelhaupt, F. M.; Baerends, E. J.; Fonseca Guerra, C.; van Gisbergen, S. J. A.; Snijders, J. G.; Ziegler, T. *J. Comput. Chem.* **2001**, *22*, 931–967.
(113) Fonseca Guerra, C.; Snijders, J. G.; te Velde, G.; Baerends, E. J. *Theor. Chem. Acc.* **1998**, *99*, 391–403.
(114) Vosko, S. H.; Wilk, L.; Nusair, M. *Can. J. Phys.* **1980**, *58*, 1200–1211.
(115) Becke, A. D. *Phys. Rev. A* **1988**, *38*, 3098–3100.
(116) Perdew, J. P. *Phys. Rev. B* **1986**, *33*, 8822–8824.
(117) Perdew, J. P. *Phys. Rev. B* **1986**, *34*, 7406.
(118) van Lenthe, E.; Baerends, E. J.; Snijders, J. G. *J. Chem. Phys.* **1993**, *99*, 4597–4610.

$N_3O_{10}P_3NaNbW_2$: C, 41.23; H, 4.23; N, 2.94. Found: C, 41.13; H, 4.53; N, 2.94.

$(P_3)Mo(N[^iPr]Ar)_3$. Solid (Mes*NPP)Nb(N[Np]Ar)$_3$ (176 mg, 0.18 mmol, 1 equiv) and P≡Mo(N[^{i}Pr]Ar)$_3$ (110 mg, 0.18 mmol, 1 equiv) were mixed, and to the mixture was added benzene (2 g). The resulting solution was transferred to a Teflon-stoppered sealable tube, which was subsequently heated to 65 °C for 3.5 h. The color remained dark-red over this time. When the solution was cooled, pale fibrous solids precipitated from it; hexane was added to facilitate the precipitation, and the solution was chilled to −35 °C. The solids were then collected atop a sintered glass frit and washed with hexane to yield an off-white fibrous solid, which was dried in vacuo (45 mg, 0.067 mmol, 37% yield). $^{31}P\{^1H\}$ NMR ($CDCl_3$, 20 °C, 121 MHz): δ −185 (br s, $\Delta\nu_{1/2}$ = 350 Hz) ppm. ^1H NMR ($CDCl_3$, 20 °C, 300 MHz): δ 6.83 (s, 3H, *p*-Ar), 6.33 (s, 6H, *o*-Ar), 4.60 (septet, 3H, *H*C(CH$_3$)$_2$), 2.28 (s, 18H, Ar−C*H*$_3$), 0.92 (d, 18H, C(C*H*$_3$)$_2$) ppm. Microanalysis and ^{13}C NMR data have appeared elsewhere.[47]

$(OC)_5W(P_3)Mo(N[^iPr]Ar)_3$. To a thawing Et_2O solution (7 mL) of [(Et_2O)Na][(OC)$_5$WP≡Nb(N[Np]Ar)$_3$] (365 mg, 0.33 mmol, 1.0 equiv) was added dropwise a thawing Et_2O solution (3 mL) of Mes*NPCl (106 mg, 0.33 mmol, 1.0 equiv), affording a color change to deep-red. The reaction mixture was allowed to stir for 1 min, and then a 22 °C solution of P≡Mo(N[^{i}Pr]Ar)$_3$ (220 mg, 0.36 mmol, 1.1 equiv) in Et_2O (4 mL) was added. This solution was stirred for 3 h at 22 °C and took on an orange hue over this time. The reaction mixture was then filtered through a bed of Celite to remove salts and concentrated to dryness in vacuo. The resulting red powder was slurried in hexane (10 mL), and the solvent was removed once more. At this point the product mixture was slurried in *n*-pentane and then chilled to −35 °C. The desired product was collected by filtration atop a sintered glass frit as a brick-red powder. The filtrate was concentrated, and this procedure was repeated several times using successively less solvent until the yellow imido and the desired red product could not be separated further. The several fractions of red powder were combined and dried in vacuo (205 mg). This material was >90% pure (the impurity was the imido **2**) as determined by NMR spectroscopy; it was further purified by storage as an *n*-pentane suspension at −35 °C followed by extraction of the undesired imido to give pure (OC)$_5$W(P$_3$)Mo(N[^{i}Pr]Ar)$_3$ as a red powder (180 mg, 0.180 mmol, 57% yield). Crystallization from toluene/Et_2O afforded analytically pure red crystals. $^{31}P\{^1H\}$ NMR (C_6D_6, 50 °C, 202.5 MHz): δ −212 (br s, $\Delta\nu_{1/2}$ = 290 Hz) ppm. ^1H NMR (C_6D_6, 20 °C, 500 MHz): δ 6.69 (s, 3H, *p*-Ar), 6.24 (br s, 6H, *o*-Ar), 4.90 (septet, 3H, *H*C(CH$_3$)$_2$), 2.10 (s, 18H, Ar−C*H*$_3$), 0.92 (br d, 18H, C(C*H*$_3$)$_2$) ppm. $^{13}C\{^1H\}$ NMR (C_6D_6, 20 °C, 125.8 MHz): δ 202.3 (quartet, J_{CP} = 12 Hz, *ax*-*C*O), 197.6 (J_{CW} = 128 Hz, *eq*-*C*O), 148.1 (*ipso*-Ar), 138.1 (Ar), 129.5 (Ar), 128.9 (br, Ar), 64.3 (br, N−*C*H(CH$_3$)$_2$), 22.6 (br, CH(*C*H$_3$)$_2$), 21.7 (Ar−*C*H$_3$) ppm. IR (*C$_6$D$_6$*, KBr) ν: 2973, 2927, 2869, 2076 (s, sharp), 1942 (vs), 1920 (s), 1600, 1586, 1153, 1113 cm^{-1}. Anal. Calcd for $C_{38}H_{48}N_3O_5P_3MoW$: C, 45.66; H, 4.84; N, 4.20. Found: C, 46.14; H, 4.90; N, 4.24.

$(OC)_5W(P_3)W(N[^iPr]Ar)_3$. To a thawing Et_2O solution (7 mL) of [(Et_2O)Na][(OC)$_5$WP≡Nb(N[Np]Ar)$_3$] (320 mg, 0.29 mmol, 1.0 equiv) was added dropwise a thawing Et_2O solution (3 mL) of Mes*NPCl (95 mg, 0.29 mmol, 1.0 equiv), affording a color change to deep-red. The reaction mixture was allowed to stir for 1 min, and then a 22 °C solution of P≡W(N[^{i}Pr]Ar)$_3$ (220 mg, 0.32 mmol, 1.1 equiv) in Et_2O (4 mL) was added. This solution was stirred for 3 h at 22 °C and took on an orange hue over this time. The reaction mixture was then filtered through a bed of Celite to remove salts and concentrated to dryness in vacuo. The resulting reddish powder was slurried in hexane (10 mL) and dried once more. At this point the reaction mixture was suspended in hexane and chilled to −35 °C for 24 h. The brick-red precipitate was collected on a sintered glass frit and dried in vacuo (160 mg, 0.15 mmol, 51% yield). $^{31}P\{^1H\}$ NMR (toluene-d_8, 40 °C, 202.5 MHz): δ −262 (br s, $\Delta\nu_{1/2}$ = 960 Hz) ppm. ^1H NMR (toluene-d_8, 40 °C, 500 MHz): δ 6.66 (s, 3H, *p*-Ar), 6.06 (br s, 6H, *o*-Ar), 4.95 (septet, 3H, *H*C(CH$_3$)$_2$), 2.09 (s, 18H, Ar−C*H*$_3$), 0.80 (br d, 18H, C(C*H*$_3$)$_2$) ppm. $^{13}C\{^1H\}$ NMR (toluene-d_8, 40 °C, 125.8 MHz): δ 199.2 (m, *ax*-*C*O), 198.1 (*eq*-*C*O), 147.2 (*ipso*-Ar), 138.1 (Ar), 129.5 (Ar), 128.8 (br, Ar), 65.8 (br, N−*C*H(CH$_3$)$_2$), 22.3 (br, CH(*C*H$_3$)$_2$), 21.7 (Ar−*C*H$_3$). IR (thin film, KBr) ν: 2066, 1933, 1917 cm^{-1}. Anal. Calcd for $C_{38}H_{48}N_3O_5P_3W_2$: C, 41.97; H, 4.45; N, 3.86. Found: C, 42.77; H, 5.07; N, 3.78.

$(AdCP_2)Mo(N[^iPr]Ar)_3$. Solid AdCP (31 mg, 0.17 mmol, 1.0 equiv) and P≡Mo(N[^{i}Pr]Ar)$_3$ (110 mg, 0.18 mmol, 1.06 equiv) were mixed and dissolved in C_6D_6 (2 mL). The resulting solution was heated to 60 °C for 3 h. After this time, ^1H and ^{31}P NMR spectra showed consumption of AdCP and the presence of **5** as the predominant species. Extraction with *n*-pentane and crystallization from toluene/*n*-pentane at −35 °C afforded pure **5** as red crystals (68 mg, 0.086 mmol, 51% yield). $^{31}P\{^1H\}$ NMR (C_6D_6, 20 °C, 202.5 MHz): δ −249 (br s) ppm. ^1H NMR (C_6D_6, 20 °C, 500 MHz): δ 6.76 (s, 6H, *o*-Ar), 6.73 (s, 3H, *p*-Ar), 4.75 (septet, 3H, C*H*), 2.21 (s, 18H, Ar−C*H*$_3$), 1.96 (m, 3H, Ad), 1.82 (m, 6H, Ad), 1.68 (m, 6H, Ad), 1.12 (d, 18H, CH(C*H*$_3$)$_2$) ppm. $^{13}C\{^1H\}$ NMR (C_6D_6, 20 °C, 125.8 MHz): δ 149.9 (*ipso*-Ar), 137.3 (Ar), 129.7 (Ar), 126.0 (Ar), 103.6 (t, J_{CP} = 79 Hz, *C*P$_2$), 58.3 (*C*H(CH$_3$)$_2$), 50.5 (Ad), 37.6 (Ad), 31.4 (Ad), 25.9 (Ad), 23.9 (CH(*C*H$_3$)$_2$), 21.8 (Ar−*C*H$_3$) ppm.

$(OC)_5W(Ph_3SnP_3)Nb(N[Np]Ar)_3$. A solution of [(12-crown-4)$_2$Na][(OC)$_5$W(P$_3$)Nb(N[Np]Ar)$_3$] (25 mg, 0.017 mmol, 1.0 equiv) and Ph_3SnCl (7 mg, 0.018 mmol, 1.06 equiv) in dimethoxyethane (5 mL) was heated to 75 °C in a Teflon-stoppered tube for 14 h. After this time, the volatiles were removed under dynamic vacuum; the residue was extracted with Et_2O, and the extract was filtered through Celite, leaving behind off-white solids. The orange filtrate was concentrated to dryness and taken up in C_6D_6 for analysis using NMR spectroscopy, which revealed a mixture containing 40% of the desired product. This mixture was further purified by extraction with $(Me_3Si)_2O$, leaving behind most of the side products and giving a solution enriched in **6** but contaminated with free HN[Np]Ar. Pure **6** was obtained in small quantities (10% yield) from the reaction of Ph_3SnCl with Na[{(CO)$_5$W}$_2$P$_3$Nb(N[Np]Ar)$_3$] at 20 °C over several days and subsequent crystallization from toluene/O(SiMe$_3$)$_2$. $^{31}P\{^1H\}$ NMR (C_6D_6, 20 °C, 201 MHz): δ −196 (br m, $\Delta\nu_{1/2}$ = 650 Hz, *P*SnPh$_3$), −235 (br, $\Delta\nu_{1/2}$ = 6500 Hz, Nb*P*$_2$W(CO)$_5$) ppm. ^1H NMR (C_6D_6, 20 °C, 500 MHz): δ 7.81 (d, 6H, J_{HSn} = 27 Hz, *o*-Ph), 7.24 (t, 6H, *m*-Ph), 7.13 (m, 3H, *p*-Ph), 6.77 (s, 6H, *o*-Ar), 6.57 (s, 3H, *p*-Ar), 3.82 (br s, 6H, N−C*H*$_2$), 2.19 (s, 18H, Ar−C*H*$_3$), 0.72 (s, 27H, ^{t}Bu) ppm. $^{13}C\{^1H\}$ NMR (C_6D_6, 20 °C, 125 MHz): δ 198.0 (br, *ax*-*C*O), 197.9 (*eq*-*C*O, J_{CW} = 130 Hz), 154.7 (br, *ispo*-Ar), 139.5, 138.6, 138.0 (J_{CSn} = 40 Hz), 136.9, 130.4, 129.6 (J_{CSn} = 56 Hz), 124.2 (br), 70.7 (br, N−*C*H$_2$), 36.5 (*C*(CH$_3$)$_3$), 29.9 (C(*C*H$_3$)$_3$), 21.9 (Ar−*C*H$_3$) ppm. Anal. Calcd for $C_{62}H_{75}N_3O_5P_3NbWSn$: C, 52.05; H, 5.28; N, 2.94; Found: C, 51.86; H, 5.28; N, 2.90.

Mes*NP(W(CO)$_5$)P$_3$Nb(N[Np]Ar)$_3$. To a thawing Et_2O solution (7 mL) of red Na[**4c**-Nb] (177 mg, 0.124 mmol) was added a thawing Et_2O solution (3 mL) of Mes*NPCl (41 mg, 1 equiv). This mixture was allowed to stir at 22 °C for 24 h, after which the mixture was chilled to −35 °C for an additional 24 h. The solution was then filtered through Celite, which was subsequently washed with *n*-pentane; the combined filtrates were concentrated to dryness in vacuo. The dried residue was then dissolved in 1:1 benzene/*n*-pentane and filtered through Celite to remove insoluble material. Another extraction with *n*-pentane followed by drying in vacuo gave a red-orange powder (158 mg, 0.115 mmol, 92% yield). $^{31}P\{^1H\}$ NMR (C_6D_6, 20 °C, 201 MHz): δ 367 (q, J_{PP} = 105 Hz, *P*NMes*), −137 (d, J_{PP} = 105 Hz, *P*$_3$Nb) ppm. ^1H NMR (C_6D_6, 20 °C, 500 MHz): δ 7.78 (s, 2H, Mes*), 6.55 (s, 3H, *p*-Ar), 6.37 (s, 6H, *o*-Ar), 3.64 (s, 6H, N−C*H*$_2$), 2.04 (s, 18H, Ar−C*H*$_3$), 1.77 (s, 18H, *o*-Mes*), 1.45 (s, 9H, *p*-Mes*), 0.77 (s, 27H, ^{t}Bu) ppm. $^{13}C\{^1H\}$ NMR (C_6D_6, 20 °C, 125.8 MHz): δ 198.6 (d, J_{CP}

(119) van Lenthe, E.; Ehlers, A.; Baerends, E. *J. Chem. Phys.* **1999**, *110*, 8943–8953.
(120) van Lenthe, E.; Baerends, E.; Snijders, J. *J. Chem. Phys.* **1994**, *101*, 9783–9792.

= 40 Hz, *ax*-*C*O), 196.3 (d, J_{CP} = 8 Hz, J_{WC} = 130 Hz, *eq*-*C*O), 153.5 (d, J_{CP} = 25 Hz, *ipso*-Mes*), 152.9 (*ipso*-Ar), 144.3 (d, J_{CP} = 5 Hz, *m*-Mes*), 138.7 (*o*-Ar), 136.7 (d, J_{CP} = 15 Hz, o-Mes*), 128.0 (Ar), 124.2 (Ar), 122.4 (Ar), 73.6 (br, N−*C*H_2), 37.0 ($CH_2C(CH_3)_3$), 35.4 (Mes*), 35.1 (Mes*), 32.8 (Mes*), 32.5 (Mes*), 30.1 ($CH_2C(CH_3)_3$), 21.8 (Ar-*C*H_3) ppm. Anal. Calcd for $C_{62}H_{89}N_4O_5P_4NbW$: C, 54.31; H, 6.54; N, 4.09; Found: C, 51.09; H, 6.24; N, 3.85.

{(OC)$_5$W}$_2$AdC(O)P$_3$Nb(N[Np]Ar)$_3$. To a thawing Et_2O solution (15 mL) of red Na[**4c**-Nb] (475 mg, 0.333 mmol) was added a thawing Et_2O solution (5 mL) of AdC(O)Cl (66 mg, 0.333 mmol). This mixture was allowed to stir for 20 min, and then the cold solution was quickly filtered through Celite; the volatiles were removed in vacuo. The solution was dried to a foam, which was quickly extracted once with Et_2O (5 mL). Upon concentration, the desired product began to precipitate from solution. The mixture was stored at −35 °C for 12 h, and the bright-red powder was isolated atop a frit. Two more crops were collected after concentration and crystallization from Et_2O, yielding a bright-red powder (300 mg, 0.19 mmol, 58% yield). $^{31}P\{^1H\}$ NMR (C_6D_6, 20 °C, 201 MHz): δ −144 (br, P_2Nb), −207 (t, J_{PP} = 180 Hz, *P*C(O)Ad) ppm. ^{1}H NMR (C_6D_6, 20 °C, 500 MHz): δ 6.65 (br, 6H, o-Ar), 6.62 (s, 1H, p-Ar), 6.56 (s, 2H, p-Ar), 4.92 (d, J = 14 Hz, 2H, CH_2), 4.60 (d, J = 14 Hz, 2H, CH_2), 2.62 (br s, 2H, CH_2), 2.22 (s, 6H, ArCH_3), 2.16 (s, 6H, Ad), 2.09 (s, 12H, ArCH_3), 1.95 (m, 3H, Ad), 1.56 (m, 6H, Ad), 0.88 (s, 18H, ^{t}Bu), 0.60 (s, 9H, ^{t}Bu) ppm. $^{13}C\{^1H\}$ NMR (C_6D_6, 20 °C, 125 MHz): δ 213.5 (d, J_{CP} = 125 Hz, (O)*C*P), 195.5 (J_{CW} = 128 Hz, *eq*-*C*O), 197.2 (J_{CP} = 33 Hz, *ax*-*C*O), 152.7 (*ipso*-Ar), 151.9 (*ipso*-Ar), 139.3 (Ar), 138.9 (Ar), 138.4 (Ar), 129.7 (Ar), 128.2 (Ar), 127.0 (Ar), 123.8 (Ar), 121.3 (Ar), 76.3 (N−*C*H_2), 60.0 (N−*C*H_2), 38.9 (Ad), 36.9 (Ad), 36.6 (*C*$(CH_3)_3$), 35.5 (*C*$(CH_3)_3$), 29.8 (Ad), 29.1 (Ad), 28.7 (C(*C*H_3)$_3$), 21.8 (Ar−*C*H_3) ppm. Elemental analysis was precluded by the thermal instability of this compound.

Kinetics of Fragmentation of 1 for Eyring Analysis. A stock solution containing (Mes*NPP)Nb(N[Np]Ar)$_3$ (135 mg) and ONb(N[Np]Ar)$_3$ (30 mg, for use as an internal standard) was prepared in C_6D_6 (5 mL) and stored at −35 °C between uses. An aliquot of this solution was transferred to a sealable (J. Young) NMR tube, which was then inserted into a prewarmed NMR probe. The temperature of the probe was verified using an ethylene glycol NMR thermometer before each run. Two- or four-scan ^{1}H NMR spectra were collected over a period of 3−5 half-lives. The integral of the methylene resonance of **1** (corrected versus the internal standard) as a function of time was fit to the first-order rate equation $I(t) = Ae^{-kt} + b$ using the automated routine of Gnuplot.[107] Three runs were performed at each temperature (except at 30 °C, where two runs were performed), and the error bars presented are at the 95% confidence level. The Eyring fit was performed using the error-weighted least-squares regression analysis of Gnuplot.

Kinetics of Fragmentation of 1-W(CO)$_5$ in the Presence of P≡Mo(N[^{i}Pr]Ar)$_3$. A thawing solution (1 mL) of Mes*NPCl (14 mg, 0.045 mmol, 1 equiv) was added to a thawing Et_2O solution (2 mL) of [Na(THF)$_3$][(CO)$_5$WP≡Nb(N[Np]Ar)$_3$] (55 mg, 0.044 mmol). The mixture was stirred for 30 s, after which the solvent was removed in vacuo. The residue was extracted with a solution of P≡Mo(N[^{i}Pr]Ar)$_3$ (37 mg, 0.060 mmol, 1.3 equiv) and ferrocene (4 mg, 0.02 mmol, used as an internal standard) in toluene-d_8 (1.0 g). The resulting extract was filtered cold through Celite into a J. Young NMR tube, which was then frozen for transport to an NMR probe precooled to 10 °C. Four-scan ^{1}H NMR spectra were collected every 248 s for 3 h. The integral of the methylene resonance of **1**-W(CO)$_5$ (corrected versus the ferrocene standard) as a function of time was fit to the first-order rate equation $I(t) = Ae^{-kt} + b$ using the automated routine of Gnuplot.[107] A rate constant (k) value of 2.1×10^{-4} s^{-1} was obtained.

Kinetics of Fragmentation of 1 in the presence of P≡Mo(N[^{i}Pr]Ar)$_3$. A solution of (Mes*NPP)Nb(N[Np]Ar)$_3$ (30 mg, 0.030 mmol) and P≡Mo(N[^{i}Pr]Ar)$_3$ (0 or 37 mg) was prepared using 1 g of C_6D_6 and transferred to a J. Young NMR tube, which was then inserted into an NMR probe prewarmed to 50 °C. Two-scan ^{1}H NMR spectra were collected every 220 s for 3 h. The integral of the methylene resonance of **1** (corrected versus residual Et_2O) as a function of time was fit to the first-order rate equation $I(t) = Ae^{-kt} + b$ using the automated routine of Gnuplot.[107] A k value of 2.5×10^{-4} s^{-1} was obtained in the presence or absence of P≡Mo(N[^{i}Pr]Ar)$_3$.

Details of X-ray Structure Determinations. Diffraction-quality crystals of **4b**-W were grown from Et_2O/*n*-pentane at −35 °C over several days, those of [(Et_2O)Na][**4c**-Nb] from benzene at room temperature, those of **5** from toluene/*n*-pentane at −35 °C, those of **6** from toluene/$(SiMe_3)_2O$ at −35 °C, and those of **7** and **8** from Et_2O at −35 °C. Crystals were mounted in hydrocarbon oil on a nylon loop or a glass fiber. Low-temperature (100 K) data were collected on a Siemens Platform three-circle diffractometer coupled to a Bruker-AXS Smart Apex CCD detector with graphite-monochromatized Mo Kα radiation (λ = 0.71073 Å) performing ϕ and ω scans. A semiempirical absorption correction was applied to the diffraction data using SADABS.[108] All of the structures were solved via direct or Patterson methods using SHELXS[109,110] and refined against F^2 on all data by full-matrix least-squares using SHELXL-97.[110,111] All of the non-hydrogen atoms were refined anisotropically. All of the hydrogen atoms were included in the model at geometrically calculated positions and refined using a riding model, and their isotropic displacement parameters were fixed at 1.2 times the U values of the atoms to which they are linked (1.5 times for methyl groups). In structures where disorders were present, the disorders were refined within SHELXL with the help of rigid-bond restraints as well as similarity restraints on the anisotropic displacement parameters for neighboring atoms and on 1,2- and 1,3-distances throughout the disordered components. The relative occupancies of disordered components were refined freely within SHELXL. Further details are provided in Table S1 and the CIF files in the Supporting Information as well as in CIF files deposited with the Cambridge Crystallographic Data Centre (CCDC).[83]

Computational Studies. All of the calculations were carried out using ADF 2004.01 (Scientific Computing and Modeling, http://www.scm.com)[112,113] on a four- or an eight-processor Quantum Cube workstation (Parallel Quantum Solutions, http://www.pqs-chem.com). In all cases, the local density approximation functional employed was that of Vosko, Wilk, and Nusair,[114] while the generalized gradient approximation was handled using the BP86 functionals of Becke and Perdew.[115–117] In addition, all of the calculations were carried out using the zero-order regular approximation for relativistic effects.[118–120] In all cases, the TZ2P (triple-ζ with two polarization functions) basis sets supplied with ADF were employed, and frozen-core approximations were made for all C atoms up to the 1s level. Geometry inputs were derived from related crystal structures and then optimized to default convergence criteria. The optimized coordinates are given in the Supporting Information.

Acknowledgment. We thank Alexander R. Fox for his contribution of P≡W(N[^{i}Pr]Ar)$_3$ and the National Science Foundation for both support of this work through Grant CHE-719157 and a predoctoral fellowship to N.A.P. We also thank Sigma-Aldrich for a donation of supplies and Thermphos International for additional financial support.

Supporting Information Available: Additional figures showing NMR spectra, variable-temperature NMR data, a kinetic plot, and a packing diagram; a table of crystal data; lists of optimized geometry coordinates; and crystallographic information files in CIF format. This material is available free of charge via the Internet at http://pubs.acs.org.

JA802080M